

Functional Aspects of Gif-Type Oxidation of Hydrocarbons Mediated by Iron Picolinate H₂O₂-Dependent Systems: Evidence for the Generation of Carbon- and Oxygen-Centered Radicals

Salma Kiani,[†] Amy Tapper,[†] Richard J. Staples,[‡] and Pericles Stavropoulos^{*,†}

Contribution from the Departments of Chemistry, Boston University, Boston, Massachusetts 02215, and Harvard University, Cambridge, Massachusetts 02138

Received January 4, 2000

Abstract: The present investigation explores the functional features of several novel and other previously ill-defined ferrous and ferric complexes of the picolinic acid anion (Pic), which are used to mediate Gif-type oxidation of hydrocarbons by H₂O₂. Complexes [Fe(Pic)₂(py)₂], [Fe(Pic)₃·0.5py], [Fe₂O(Pic)₄(py)₂], [Fe₂(μ-OH)₂(Pic)₄], and FeCl₃ have been employed in oxygenations of adamantane by H₂O₂ mostly in py/AcOH to reveal that *tert*- and *sec*-adamantyl radicals are generated in Gif solutions. The alleged absence of *sec*-adamantyl radicals from Gif product profiles has been previously interpreted as compelling evidence in support of a non-radical mechanism for the activation of secondary C–H sites in Gif chemistry. The product profile is entirely dictated by trapping of the diffusively free adamantyl radicals, since authentic *tert*- and *sec*-adamantyl radicals are shown to partition between dioxygen and protonated pyridine at 4% O₂ (in N₂), or between dioxygen and TEMPO at 100% O₂, in a manner analogous to that observed in Gif oxygenations of adamantane. The low *tert*/*sec* selectivity (2.2–4.5) obtained, increasing with increasing dioxygen partial pressure, and the small intramolecular kinetic isotope effect values revealed by employing adamantane-1,3-*d*₂ (1.06(6) (Ar); 1.73(2) (4% O₂ in N₂)), indicate the presence of an indiscriminate oxidant under inert atmosphere, coupled to a more selective oxidant at higher partial pressures of dioxygen. Gif oxygenation of DMSO by H₂O₂ mediated by [Fe(Pic)₂(py)₂] provides pyridine-trapped methyl radicals under argon, as expected for the addition reaction of hydroxyl radicals to DMSO. The reaction is progressively inhibited by increasing amounts of EtOH, generating pyridine-captured CH₃•CHOH and •CH₂CH₂OH radicals. Quantification of the DMSO- versus EtOH-derived alkyl radicals affords an estimate of $k_{\text{EtOH}}/k_{\text{DMSO}}$ equal to 0.34(3), in reasonable agreement with the kinetics of radiolytically produced hydroxyl radicals ($k_{\text{EtOH}}/k_{\text{DMSO}} = 0.29$). The formation of methyl radicals in Gif oxygenation of DMSO is also supported by the quantitative generation of *tert*-adamantyl radicals in the presence of 1-iodoadamantane. These results are consistent with the action of hydroxyl radicals in Gif oxygenations by Fe^{II/III}/H₂O₂ (Ar), most likely coupled to substrate-centered alkoxy radicals under O₂. The oxygen-centered radicals perform H-atom abstractions from Gif substrates to generate diffusively free carbon-centered radicals, in accord with previously reported findings.

Introduction

Early versions of Gif-type hydrocarbon-oxidizing systems¹ were composed of an Fe^{II/III} complex, a reducing agent (Fe, Zn, electrochemical cathode) and dioxygen (or air), operating primarily in a pyridine/carboxylic acid matrix (10:1 v/v).² More recently, Gif reagents have been represented by Fe^{III}/H₂O₂ or Fe^{III}/*t*-BuOOH (60 °C) combinations,³ frequently assisted by the presence of 2-picolinic acid (PicH) to enhance the rate of catalytic oxygenations.⁴ A typical system employed by Barton to accumulate most of the mechanistic data known to date involves the combination of FeCl₃/PicH/H₂O₂ (1:4:4) in pyridine or py/AcOH.³ A closely related reagent, Fe(Pic)₂/H₂O₂ (or

t-BuOOH) (1:20) in py/AcOH (2:1),^{4b} has been proposed by Sawyer⁵ to mediate “oxygenated Fenton” chemistry. Although the presumed active oxidants are differently formulated (a high-valent Fe^V=O unit in Gif¹ and an unusual [Fe(OOR)(O₂)(Pic)₂-(pyH⁺)] species in oxygenated Fenton chemistry⁵), both systems have been interpreted to perform oxygenation of substrates via pathways that, with a few exceptions, do not involve oxygen- or carbon-centered radicals.

One argument in support of the non-radical mechanism in Gif chemistry is the alleged selectivity for the oxygenation of secondary positions (leading primarily to ketones) over tertiary or primary sites (*sec* > *tert* > *prim*).⁶ This unusual selectivity (which in our hands has been confirmed for isopentane,⁷ albeit

[†] Boston University.

[‡] Harvard University.

(1) (a) Barton, D. H. R.; Doller, D. *Acc. Chem. Res.* **1992**, *25*, 504–512. (b) Barton, D. H. R. *Aldrichim. Acta* **1990**, *23*, 3–11.

(2) Barton, D. H. R.; Bévière, S. D.; Chavasiri, W.; Cshai, E.; Doller, D.; Liu, W.-G. *J. Am. Chem. Soc.* **1992**, *114*, 2147–2156.

(3) Barton, D. H. R.; Hu, B.; Taylor, D. K.; Rojas Wahl, R. U. *J. Chem. Soc., Perkin Trans. 2* **1996**, 1031–1041.

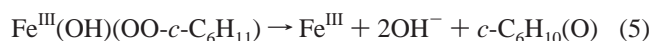
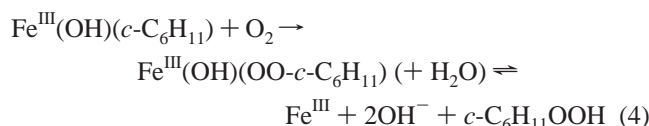
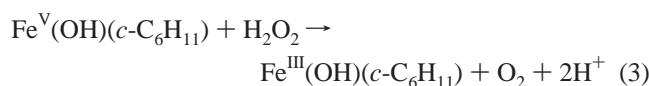
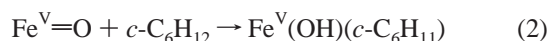
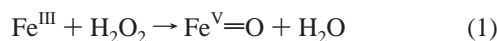
(4) (a) Balavoine, G.; Barton, D. H. R.; Boivin, J.; Gref, A. *Tetrahedron Lett.* **1990**, *3*, 659–662. (b) Tung, H.-C.; Kang, C.; Sawyer, D. T. *J. Am. Chem. Soc.* **1992**, *114*, 3445–3455.

(5) Sawyer, D. T.; Sobkowiak, A.; Matsushita, T. *Acc. Chem. Res.* **1996**, *29*, 409–416.

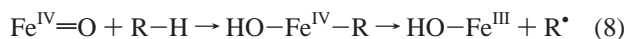
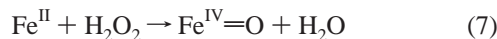
(6) (a) Barton, D. H. R.; Boivin, J.; Gastiger, M.; Morzycki, J.; Hay-Motherwell, R. S.; Motherwell, W. B.; Ozbalik, N.; Schwartztruber, K. M. *J. Chem. Soc., Perkin Trans. 1* **1986**, 947–955. (b) Barton, D. H. R.; Doller, D.; Ozbalik, N.; Balavoine, G.; Gref, A. *Tetrahedron Lett.* **1990**, *31*, 353–356. (c) Barton, D. H. R.; Chavasiri, W. *Tetrahedron* **1997**, *53*, 2997–3004.

(7) Singh, B.; Long, J. R.; Fabrizi de Biani, F.; Gatteschi, D.; Stavropoulos, P. *J. Am. Chem. Soc.* **1997**, *119*, 7030–7047.

at such low yields as to warrant caution) has been accounted for by a general mechanism¹ (eqs 1–6; illustrated for cyclohexane) that involves concerted [2 + 2] addition of C–H bonds across high-valent Fe^V=O units (eqs 1, 2). The proposed four-atom centered intermediate would thus favor *sec*-C–H oxygenation as a compromise between steric encumbrance and C–H bond strength. Another important fact taken into account in the formulation of the Barton mechanism is the detection of cyclohexylhydroperoxide² (eq 4), eventually decomposing via metal-dependent steps to yield cyclohexanone (major product) and cyclohexanol (minor product) (eqs 5, 6). The important observation by M. J. Perkins⁸ that the oxygen incorporated in cyclohexylhydroperoxide is derived from dioxygen, raised the question whether the immediate precursor to the alkylhydroperoxide (ROOH) is actually free alkylperoxyl radical (ROO•). The latter will be generated by the reaction of diffusively free alkyl radicals (R•) with internally produced or externally provided dioxygen. A non-radical version of the sequence of events leading to the formation of the alkylhydroperoxide has been accommodated in Barton's mechanism by assuming metal-bound alkyl (eq 3) and alkylperoxo moieties (eq 4).



In addition to Fe(III)/H₂O₂ based Gif-type reagents that give rise to the non-radical “Fe^{III}/Fe^V manifold” noted above, Barton has also recognized³ the existence of an independent “Fe^{II}/Fe^{IV} manifold”, generated by circumstantial Fe(II)/H₂O₂ interactions, that yields alkyl radicals via eqs 7 and 8.



The applicability of a non-radical mechanism has been experimentally challenged, primarily for those branches of Gif⁹ and “oxygenated Fenton”¹⁰ systems (as well as other biomimetically designed hydrocarbon-oxidizing reagents¹¹) employing *t*-BuOOH and other diagnostic alkylhydroperoxides. Compelling evidence provided for these systems by Minisci^{9a,12}

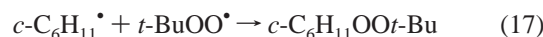
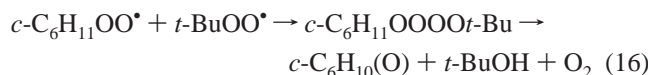
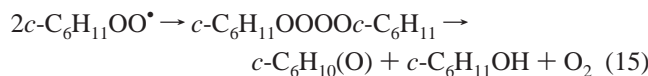
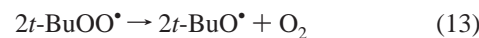
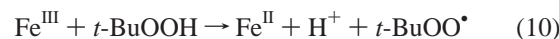
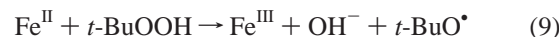
(8) Knight, C.; Perkins, M. J. *J. Chem. Soc., Chem. Commun.* **1991**, 925–927.

(9) (a) Minisci, F.; Fontana, F.; Araneo, S.; Recupero, F.; Zhao, L. *Synlett* **1996**, 119–125. (b) Snelgrove, D. W.; MacFaul, P. A.; Ingold, K. U.; Wayner, D. D. M. *Tetrahedron Lett.* **1996**, 37, 823–826.

(10) MacFaul, P. A.; Wayner, D. D. M.; Ingold, K. U. *Acc. Chem. Res.* **1998**, 31, 159–162.

(11) Arends, I. W. C. E.; Ingold, K. U.; Wayner, D. D. M. *J. Am. Chem. Soc.* **1995**, 117, 4710–4711. (b) MacFaul, P. A.; Arends, I. W. C. E.; Ingold, K. U.; Wayner, D. D. M. *J. Chem. Soc., Perkin Trans. 2* **1997**, 135–145. (c) MacFaul, P. A.; Ingold, K. U.; Wayner, D. D. M.; Que, L., Jr. *J. Am. Chem. Soc.* **1997**, 119, 10594–10598.

and Ingold^{9b,10,11} lends credence to a typical Haber–Weiss–Walling¹³ radical mechanism (eqs 9–17), featuring involvement of *t*-BuO•/*t*-BuOO• radicals and substrate-centered alkyl/alkylperoxyl radicals. This pathway is usually suspected by account of a one/2-ol ratio of ≥ 1 (typical values tend to be close to 1) owing to Russell¹⁴ decomposition of alkylperoxyl radicals (eqs 15, 16). In addition, mixed alkyl(*tert*-butyl)peroxides are observed^{11c} in good yields (eq 17). Other diagnostic elements of alkoxy radical (RO•) involvement as the hydrogen abstracting agent include observation of byproducts of β -scission and intramolecular hydrogen abstraction,^{13a} as well as trapping of RO•/ROO• radicals by analogues of vitamin E (α -tocopherol)¹⁵ or diphenylamine.¹⁰ Following Barton's reappraisal¹⁶ of the chemistry of *t*-BuOOH-based Gif systems, there is now consensus that the main role of these Fe(II)/Fe(III) reagents is to generate *t*-BuO•/*t*-BuOO• radicals (eqs 9, 10).



The unusually high one/2-ol ratio (~ 3 –10) obtained in Gif oxygenations of *sec*-C–H positions (cyclohexane, adamantane) indicates that, in addition to eqs 15 and 16, decomposition of *sec*-alkylperoxyl radicals may take place via metal-dependent pathways. In Barton's mechanism,¹ the enhancement of ketone production is attributed to formation and decay of Fe(III)–alkylperoxy intermediates (eqs 4, 5) in a non-radical mechanism. More recently, a general argument concerning the non-applicability of the Haber–Weiss–Walling mechanism for the Fe(II)-dependent decomposition of secondary and primary (as opposed to tertiary) alkylhydroperoxides has been proposed by Barton¹⁷ to explain that not much alcohol is obtained in pyridine solutions. In other solvents (CH₃CN/AcOH, AcOH/H₂O), the

(12) (a) Minisci, F.; Fontana, F.; Araneo, S.; Recupero, F.; Banfi, S.; Quici, S. *J. Am. Chem. Soc.* **1995**, 117, 226–232. (b) Minisci, F.; Fontana, F.; Araneo, S.; Recupero, F. *J. Chem. Soc., Chem. Commun.* **1994**, 1823–1824. (c) Minisci, F.; Fontana, F. *Tetrahedron Lett.* **1994**, 35, 1427–1430.

(13) (a) Walling, C. *Acc. Chem. Res.* **1998**, 31, 155–157. (b) Walling, C. *Acc. Chem. Res.* **1975**, 8, 125–131.

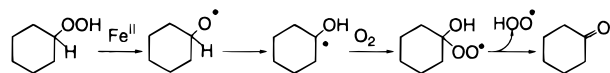
(14) Russell, G. A. *J. Am. Chem. Soc.* **1957**, 79, 3871–3877.

(15) (a) Evans, C.; Scaiano, J. C.; Ingold, K. U. *J. Am. Chem. Soc.* **1992**, 114, 4589–4593. (b) Valgimigli, L.; Banks, J. T.; Ingold, K. U.; Luszyk, J. *J. Am. Chem. Soc.* **1995**, 117, 9966–9971. (c) Burton, G. W.; Ingold, K. U. *Acc. Chem. Res.* **1986**, 19, 194–201.

(16) (a) Barton, D. H. R. *Synlett* **1997**, 229–230. (b) Barton, D. H. R.; Le Gloahec, V. N.; Patin, H.; Launay, F. *New J. Chem.* **1998**, 22, 559–563. (c) Barton, D. H. R.; Le Gloahec, V. N.; Patin, H. *New J. Chem.* **1998**, 22, 565–568.

(17) Barton, D. H. R.; Launay, F. *Tetrahedron* **1997**, 53, 14565–14578.

Scheme 1



amount of alcohol generated is comparable to that of ketone. However, the alternative radical proposition¹⁸ of pyridine-facilitated 1,2-hydrogen shift¹⁹ (Scheme 1) merits further consideration.

The propensity of *t*-BuOOH supported oxygenation systems²⁰ to generate *t*-BuO[•]/*t*-BuOO[•] radicals even in cases in which high-valent iron-oxo units are otherwise regarded to play a prominent role (for instance, in shunt pathways of P-450²¹), raises doubt whether these systems can be used as representative indicators of mechanism for other mainstream Gif reagents. Mechanistic insights regarding Gif systems employing H₂O₂ or O₂/Zn have been put forward by M. J. Perkins²² in a lucid reinterpretation (vide infra) of Barton's results, hinting toward an oxygen- and carbon-centered radical mechanism for the totality of Gif chemistry. However, unequivocal detection and quantification of the aforementioned radicals in these systems is currently resting on insufficient experimental evidence. A notable exception is an elegant study by M. Newcomb and co-workers,²³ in which an ultrafast radical-clock probe has been used to distinguish between pathways adopted by biological monooxygenases (P-450,²⁴ sMMO²⁵) and a Gif-type reagent (FeCl₃ in py/AcOH), as indicated by the generation of short-lived (<100 fs) and diffusively free alkyl radicals, respectively. These results have been interpreted by Barton as exceptional cases of alkyl radical formation via homolytic Fe^V-R cleavage, similar to those obtained for the tertiary positions of the strained hydrocarbons adamantane² and decalin.^{6a}

In the present article, we report that two well-characterized iron picolinate precursor species, ferrous [Fe(Pic)₂(py)₂] and ferric [Fe(Pic)₃]·0.5py, frequently used as mediators of "oxygenated Fenton"^{4b} and Gif chemistry³ respectively, enable oxygenation of adamantane by H₂O₂ that demonstrates formation of not only tertiary adamantyl radicals, as previously recognized,² but also of secondary adamantyl radicals. The alleged absence of the latter has been central to Barton's argument¹ in support of a non-radical mechanism. Other Gif-type reagents ([Fe₂O(Pic)₄(py)₂], FeCl₃, [Fe₂(μ-OH)₂(Pic)₄]) also perform adamantane oxidations in which *sec*-adamantyl radicals are

(18) We thank a reviewer for proposing this alternative radical pathway.

(19) 1,2-Hydrogen migrations are more common in aqueous solutions, see: Beckwith, A. L. J.; Ingold, K. U. In *Rearrangements in Ground and Excited States*; de Mayo, P., Ed.; Academic Press: New York, 1980; Vol. 1, pp 161–310.

(20) (a) Nguyen, C.; Guajardo, R. J.; Mascharak, P. K. *Inorg. Chem.* **1996**, *35*, 6273–6281. (b) Rabion, A.; Chen, S.; Wang, J.; Buchanan, R. M.; Seris, J.-L.; Fish, R. H. *J. Am. Chem. Soc.* **1995**, *117*, 12356–12357.

(21) (a) Meunier, B. *Chem. Rev.* **1992**, *92*, 1411–1456. (b) Mansuy, D.; Bartoli, J.-F.; Momenteau, M. *Tetrahedron Lett.* **1982**, *23*, 2781–2784. (c) Mansuy, D.; Bartoli, J.-F.; Chottard, J.-C.; Lange, M. *Angew. Chem., Int. Ed. Engl.* **1980**, *19*, 909–910. (d) Ledon, H. C. R. *Hebd. Seances Acad. Sci., Ser. C* **1979**, *288*, 29–31. (e) Baccouche, M.; Ernst, J.; Fuhrhop, J.-H.; Schlözer, R.; Arzoumanian, H. *J. Chem. Soc., Chem. Commun.* **1977**, 821–822.

(22) Perkins, M. J. *J. Chem. Soc. Rev.* **1996**, 229–236.

(23) Newcomb, M.; Simakov, P. A.; Park, S.-U. *Tetrahedron Lett.* **1996**, *37*, 819–822.

(24) (a) Newcomb, M.; Le Tadic-Biadatti, M.-H.; Chestney, D. L.; Roberts, E. S.; Hollenberg, P. F. *J. Am. Chem. Soc.* **1995**, *117*, 12085–12091. (b) Atkinson, J. K.; Hollenberg, P. F.; Ingold, K. U.; Johnson, C. C.; Le Tadic, M.-H.; Newcomb, M.; Putt, D. A. *Biochemistry* **1994**, *33*, 10630–10637.

(25) (a) Choi, S.-Y.; Eaton, P. E.; Hollenberg, P. F.; Liu, K. E.; Lippard, S. J.; Newcomb, M.; Putt, D. A.; Upadhyaya, S. P.; Xiong, Y. *J. Am. Chem. Soc.* **1996**, *118*, 6547–6555. (b) Liu, K. E.; Johnson, C. C.; Newcomb, M.; Lippard, S. J. *J. Am. Chem. Soc.* **1993**, *115*, 939–947.

involved. Furthermore, by using suitable substrates (dimethyl sulfoxide, ethanol) and competition kinetics, we provide compelling evidence that the hydrogen-abstracting agent is hydroxyl radicals under inert atmosphere, coupled to a more selective oxidant (most likely adamantyloxy radicals) in the presence of dioxygen.

Among other novel features, an important aspect of the present systematic exploration is the employment of *mainstream* Gif reagents and substrates to unravel product profiles which frequently are in disagreement with experimental data on the basis of which mechanistic interpretations have been put forward by Barton and co-workers.^{2,3} Thus, this work substantiates Perkins' "radical reappraisal"²² of Gif chemistry by means of expanding and amending the experimental record, as well as by employing a handful of new diagnostic substrates to directly interrogate the nature of the active oxidant(s) involved in H₂O₂-dependent Gif chemistry. The notion that specialized substrates such as Newcomb's radical clocks,²³ should be treated as exceptional instances, can no longer be maintained, as generation of carbon-centered radicals is shown here to pervade the most common reagents and substrates used in Gif chemistry.

Experimental Section

Preparation of Compounds. All operations were performed under a pure dinitrogen or argon atmosphere, using Schlenk techniques on an inert gas/vacuum manifold or in a drybox (O₂, H₂O <1 ppm). Hexane, petroleum ether, and toluene were distilled over Na, and THF and diethyl ether, over Na/Ph₂CO. Acetonitrile and methylene chloride were distilled over CaH₂. Ethanol and methanol were distilled over the corresponding magnesium alkoxide, and acetone, over drierite. Anhydrous pyridine, dimethyl sulfoxide and dimethyl formamide (water < 0.005%) and double-distilled acetic acid (metallic impurities in parts-per-trillion) were purchased from Aldrich. Deuterated solvents for NMR experiments were purchased from Cambridge Isotope Laboratory. All solvents, with the exception of methanol and water were degassed by three freeze-pump-thaw cycles. Methanol and water were degassed by bubbling nitrogen or argon for 0.5 h. Starting materials were purchased from Aldrich and are of the highest available purities.

[Fe(Pic)₂]_n (1). A mixture of Fe powder (99.99%, 160 mg, 2.86 mmol) and picolinic acid (665 mg, 5.40 mmol) was stirred in CH₂Cl₂ (50 mL) for 4 days under nitrogen in an inert-atmosphere drybox. The red-orange solution was then filtered from any remaining Fe, and excess diethyl ether was added to the filtrate to precipitate the red powder of **1** (540 mg, 63%). ¹H NMR (CD₂Cl₂): δ 35.62, 47.08, 58.93. IR (KBr): ν_{OCO} 1653, 1594, 1576 cm⁻¹. Anal. Calcd for C₁₂H₈N₂FeO₄: C, 48.04; H, 2.69; N, 9.34. Found: C, 48.24; H, 2.71; N, 9.42.

[Fe(Pic)₂(py)₂] (2). A mixture of Fe powder (99.99%, 160 mg, 2.86 mmol) and picolinic acid (665 mg, 5.40 mmol) was suspended in pyridine (50 mL). The reaction mixture was stirred for 4 days in a nitrogen-atmosphere glovebox. Unreacted Fe powder was filtered off and diethyl ether was slowly diffused into the filtrate to afford a brick red microcrystalline solid (650 mg, 50%). Efforts to obtain X-ray quality crystals of this compound were unsuccessful. ¹H NMR (CD₂Cl₂): δ 7.58–8.69 (m), 18.77 (br, 2H, 2H-py), 35.37 (br, 1H, 4H-Pic), 46.69 (br, 1H, 3H-Pic), 58.67 (br, 1H, 5H-Pic), 138.53 (br, 6H-Pic). IR (KBr): ν_{OCO} 1645, 1594, 1348 cm⁻¹. UV-vis (py): λ_{max} = 428 (ε_m = 2800) nm. Anal. Calcd for C₂₂H₁₈N₄FeO₄: C, 57.56; H, 3.96; N, 12.23. Found: C, 57.60; H, 3.98; N, 12.39.

[Fe(Pic)(py)₃Cl] (3). Recrystallization of **2** from a mixture of pyridine and methylene chloride (1:1 v/v) affords red crystals of **3** and white needle-shaped crystals of 1,1'-methylene-bispyridinium dichloride ([C₅H₅N-CH₂-NC₅H₅]Cl₂). The latter compound is also obtained from a mixture of py/CH₂Cl₂ (1:1 v/v) in the absence of metal. IR(KBr): ν_{OCO} 1634, 1601, 1530, 1483, 1442. Anal. Calcd for C₂₁H₁₉N₄Cl₁-Fe₁O₂: C, 55.96; H, 4.25; N, 12.43. Found: C, 55.60; H, 4.32; N, 12.52.

[Fe₂(Pic)₄(4-*tert*-Bupy)₂] (4). Compound **1** (100 mg, 0.33 mmol) was dissolved in 4-*tert*-butylpyridine (10.0 mL) to afford a deep red

solution. Diethyl ether was slowly diffused to the filtrate of the solution to yield carmine red microcrystals of **4** (123 mg, 86%). ¹H NMR (CD₂Cl₂): δ 1.08 (s, 9H, C(CH₃)₃), 6.2–8.4 (m), 11.82 (br, 2H, 2H-py) 25.60 (br, 2H, 4H-Pic), 45.56 (br, 2H, 3H-Pic), 60.41 (br, 2H, 5H-Pic), 118.48 (br, 6H-Pic). IR (KBr): ν_{OCO} 1640, 1610, 1550, 1490 cm⁻¹. Anal. Calcd. for C₄₂H₄₂N₆Fe₂O₈: C, 57.94; H, 4.86; N, 9.65. Found: C, 57.48; H, 4.79; N, 9.95.

[Fe₂(Pic)₄(DMF)₂] (**5**). Quantitative amounts of this compound were obtained by dissolving **1** in dimethylformamide (DMF), or better **2** (200 mg, 0.44 mmol) in 30.0 mL of DMF. Red crystals of **5** (137 mg, 83%) suitable for X-ray analysis were grown by diffusion of diethyl ether into DMF at 0 °C. ¹H NMR ((CD₃)₂NCDO): δ 36.2 (br, 1H, 4H-Pic), 46.5 (br, 1H, 3H-Pic), 59.9 (br, 1H, 5H-Pic), 137.5 (br, 6H-Pic). IR (KBr): ν_{OCO} 1642, 1575, 1320, 1270 cm⁻¹. UV-vis (DMF): λ_{max} = 462 (ε_m = 1120) nm. Anal. Calcd for C₃₀H₃₀N₆Fe₂O₁₀: C, 48.28; H, 4.05; N, 11.26. Found: C, 48.36; H, 4.12; N, 11.38.

[Fe(Pic)₂(MeOH)₂] (**6**). Solid [Fe(Pic)₂]_n (**1**, 200 mg, 0.67 mmol) was dissolved in freshly degassed methanol (15.0 mL). The solution was filtered and allowed to stand at room temperature over a period of one week, upon which large red-plate crystals (180 mg, 74%) suitable for X-ray analysis were obtained. ¹H NMR (CD₂Cl₂): δ 3.39 (br, 1H, MeOH), 3.75 (br, 3H, CH₃OH), 23.94 (br, 1H, 4H-Pic), 45.57 (br, 1H, 3H-Pic), 62.20 (br, 1H, 5H-Pic). IR (KBr): ν_{OCO} 1624, 1589, 1564, 1444 cm⁻¹. Anal. Calcd for C₁₄H₁₆N₂Fe₁O₆: C, 46.18; H, 4.43; N, 7.69. Found: C, 45.96; H, 4.56; N, 7.70.

[Fe₂O(Pic)₄(py)₂] (**8**). This compound was generated in solution by dissolving **9** (80 mg, 0.11 mmol) in pyridine (20.0 mL). Careful layering of diethyl ether onto pyridine affords light brown solid of analytically pure **8** (72 mg, 84%) upon standing at ambient temperature. ¹H NMR (CD₂Cl₂): δ 7.71 (br), 9.07 (br), 111.30 (br), 125.22 (br). IR (KBr): ν_{OCO} 1654, 1569, 1351, 1475, ν_{FeOFe} 856 cm⁻¹. UV-vis (py): λ_{max} = 350 (ε_m = 8000) nm. Anal. Calcd for C₃₄H₂₆N₆Fe₂O₉: C, 52.75; H, 3.38; N, 10.85. Found: C, 52.95; H, 3.38; N, 10.84.

[Fe₂O(Pic)₄(DMF)₂] (**9**). Solid **2** (100 mg, 0.22 mmol) was dissolved in 20.0 mL of DMF. This solution was then exposed to dry oxygen for 30 min at room temperature. The color of the solution changed from dark red to brown. X-ray quality crystals of **9** (68 mg, 82%) were obtained by diffusing diethyl ether into the DMF solution at 0 °C. ¹H NMR (CD₂Cl₂): δ 2.75 (br), 2.89 (br), 7.95 (br), 111.01 (br), 123.30 (br). IR (KBr): ν_{OCO} 1653, 1344, 1288, ν_{FeOFe} 867 cm⁻¹. UV-vis (DMF): λ_{max} = 350 (ε_m = 7500) nm. Anal. Calcd for C₃₀H₃₀N₆Fe₂O₁₁: C, 47.27; H, 3.97; N, 11.02. Found: C, 47.39; H, 3.97; N, 11.08.

[Fe(Pic)₃]_{0.5py} (**10**). A mixture of picolinic acid (6.15 g, 0.05 mol) and sodium hydroxide (2.0 g, 0.05 mol) in 10.0 mL of water was slowly added to a slurry of Fe₂(SO₄)₃ (3.3 g, 0.008 mol) in 100 mL of acetonitrile. The reaction mixture was stirred for 2 h, followed by filtration and extraction of the precipitate with 3 × 60 mL of acetonitrile. The combined organic layers were dried over MgSO₄. Removal of solvent under vacuum afforded 2.8 g (40%) of crude [Fe(Pic)₃]. Yellow crystals of the pyridine-solvated adduct **10**, suitable for X-ray analysis, were grown by diffusing diethyl ether into a pyridine solution of the crude product (see text for other preparation methods). ¹H NMR (CD₂Cl₂): δ 7.4 (br), 7.7 (br), 8.7 (br), 109.72 (br), 123.67 (br). IR (KBr): ν_{OCO} 1676, 1604, 1576, 1326, 1287 cm⁻¹. UV-vis (py): λ_{max} = 341 (2580) nm. Anal. Calcd for C_{20.5}H_{14.5}N_{3.5}Fe₁O₆: C, 53.27; H, 3.16; N, 10.60. Found: C, 53.11; H, 3.09; N, 10.47.

[Fe₂(μ-OMe)₂(Pic)₄] (**11**). Compound [Fe₂(μ-OH)₂(Pic)₄] (100 mg, 0.16 mmol) was dissolved in methanol (20.0 mL) upon mild heating. Yellow-green plate-shaped crystals of **11** (85 mg, 81%) were obtained by slow crystallization from methanol at room temperature. IR (KBr): ν_{OCO} 1672, 1604, 1473, 1331, 1286 cm⁻¹. UV-vis (MeOH): λ_{max} = 251 (ε_m = 1400) nm. Anal. Calcd for C₂₆H₂₂N₄Fe₂O₁₀: C, 47.16; H, 3.35; N, 8.46. Found: C, 47.43; H, 3.28; N, 8.57.

Catalytic Oxidations. A typical oxidation of substrate (adamantane) mediated by various iron-containing species (**2**, **8**, **10**, FeCl₃, [Fe₂(μ-OH)₂(Pic)₄]) was conducted as follows. In a 50.0 mL round-bottom flask, the iron reagent (0.20 mmol) was dissolved under anaerobic conditions in 30.0 mL of pyridine and 3.0 mL of acetic acid followed by addition of adamantane (681 mg, 5.0 mmol). Degassed aqueous solution (30%) of hydrogen peroxide (0.24 mL, 2.0 mmol) was added

using a syringe-pump over a period of 6 h upon vigorous stirring. The oxidations were performed under inert atmosphere (N₂ or Ar) and/or under various partial pressures of dioxygen (O₂ (4%) in N₂, air, O₂ (100%)). Other variables included addition of picolinic acid (0.2 or 16.0 mmol) and/or Zn (20.0 mmol) to the reaction mixture. Occasionally, acetic acid was omitted from the solvent matrix. When TEMPO was used in experiments directed toward trapping of adamantyl radicals, the exact procedure noted above was followed with the addition of TEMPO (2.0 or 5.0 mmol, as specified).

Catalytic oxidations of DMSO and EtOH were conducted under the general conditions noted in oxidations of adamantane, employing amounts specified in Table 4. In the case of oxidations in the presence of 1-iodoadamantane (1.31 g, 5.0 mmol), the reaction and follow-up procedure were protected from light exposure but were otherwise performed as indicated for the other substrates, using amounts of materials as specified in the text.

The workup procedure for identification and quantification of products of adamantane oxidation was performed as follows. Excess oxalic acid (5 equiv over iron) and triphenylphosphine (2 equiv over H₂O₂) were occasionally added at the end of the reaction to ensure complexation of iron to inert iron-oxalato species, and reduction of any remaining H₂O₂ and adamantylhydroperoxides to water and corresponding alcohols, respectively. The internal standard (hexamethylbenzene or 1,3,5-trisopropylbenzene) was added to the reaction mixture, and an aliquot (2 mL) was withdrawn for GC or GC-MS analysis. After addition of water (3 mL), the aliquot was extracted with diethyl ether (3 × 5 mL). The combined diethyl ether layers were dried over magnesium sulfate. The samples were analyzed by a Hewlett-Packard 5890 Series II Capillary GC, employing Supelco SPB-1 or SPB-50 capillary columns (30 m (length), 0.32 mm (i.d.), 0.25 μm (d_f)), a flame ionization detector, and a Hewlett-Packard 3395 integrator. The following was a typical temperature program for the SPB-1 column: initial temperature = 50 °C; hold temperature for 9 min; increase temperature by 3 °C/min up to 135 °C, thereafter by 5 °C/min up to the final temperature 260 °C. Products were identified by their respective retention times versus authentic samples and by mass determination on a Finnigan MAT-90 MS coupled to a Varian 3400 GC. Adamantane and authentic oxygenated adamantane products (1-Ad-ol, 2-Ad-ol, 2-Ad-one) as well as 1-chloroadamantane were purchased from Aldrich. 2-Chloroadamantane was a gift from Barton's group. Authentic *tert*-adamantylpyridines (2-(1-Ad)-py, 4-(1-Ad)-py),²⁶ *sec*-adamantylpyridines (2-(2-Ad)-py, 4-(2-Ad)-py),²⁶ 1-Ad-TEMPO,²⁷ and 2-Ad-TEMPO²⁷ were prepared by photolysis of suitable adamantyl-radical generating precursors in the presence of protonated pyridine or TEMPO according to literature procedures.

The follow-up analytical procedure for quantification of the pyridine-trapped alkyl radicals, generated in oxidations of DMSO and EtOH, is similar to the one noted above, with the exception that the reaction aliquot was rendered alkaline (NaOH 20% w/v) prior to extraction by diethyl ether. Furthermore, a Hewlett-Packard Carbowax column (30 m (length), 0.50 mm (i.d.), 0.25 μm (d_f)) was employed under a temperature program identical to that noted above, with the exception that the final temperature was set at 220 °C. Authentic 2-, 3-, 4-picolines, 2-(2-CH₂CH₂OH)py, and 4-(2-CH₂CH₂OH)py were purchased from Aldrich. (±)-α-Methyl-4-pyridinemethanol was purchased from Fluka. A specimen of the corresponding (±)-α-methyl-2-pyridinemethanol was unavailable, and this important compound was quantified using the isomer 2-(2-CH₂CH₂OH)py as equivalent authentic sample.

Control Experiments Involving Authentic Adamantyl Radicals. Barton's esters of *N*-hydroxypyridine-2-thione²⁶ with 1-adamantanecarboxylic acid and 2-adamantanecarboxylic acid²⁸ (0.115 mmol of each) were dissolved in a mixture of pyridine (10.0 mL) and acetic acid (1.0 mL). The iron reagents [Fe(Pic)₂(py)₂] (**2**) (4.2 mg, 9.2 μmol) or [Fe(Pic)₃]_{0.5py} (**10**) (4.3 mg, 9.2 μmol) were added, and the mixture was subjected to photolysis for 2 h by means of an ACE-Hanovia high-

(26) Barton, D. H. R.; Halley, F.; Ozbalik, N.; Schmitt, M.; Young, E.; Balavoine, G. *J. Am. Chem. Soc.* **1989**, *111*, 7144–7149.

(27) Barton, D. H. R.; Bévière, S. D.; Chavasiri, W.; Doller, D.; Liu, W.-G.; Reibenspies, J. H. *New J. Chem.* **1992**, *16*, 1019–1029.

(28) Farcasius, D. *Synthesis* **1972**, 615–616.

pressure mercury-vapor lamp, while the solution was continuously purged by O₂ (4%) in N₂. The same procedure was employed in those experiments in which TEMPO (0.500 mmol) was added, with the exception that 0.250 mmol of each ester was used and pure O₂ was bubbled through the solution under photolysis. In all cases, the product profile was analyzed by GC and GC-MS as indicated above.

Kinetic Isotope Effect (KIE) Measurements. The intermolecular deuterium kinetic isotope effect was measured for adamantane by conducting catalytic oxidations on a mixture of adamantane/adamantane-*d*₁₆ (1:1). The following was a typical procedure. The iron reagent, [Fe(Pic)₂(py)₂] (**2**) (9.2 mg, 0.02 mmol) or [Fe(Pic)₃]-0.5py (**10**) (9.2 mg, 0.02 mmol), and adamantane (0.25 mmol)/adamantane-*d*₁₆ (0.25 mmol) were dissolved in a mixture of pyridine (3.0 mL) and acetic acid (0.3 mL). Aqueous H₂O₂ (30%, 30 μL, 0.2 mmol) was added to this stirred solution via a syringe pump over a period of 6 h under argon (delivered to the headspace of the flask under static conditions). Throughout the experiment, the mixture was maintained at 25.0(1) °C with the aid of a Brinkman RM6 thermostat. The workup procedure was performed in a manner similar to that described for adamantane oxidations. KIE values were obtained for each product from the ratio of the corresponding protio/deuterio product yield (average of three trials), evaluated by GC separation of all products and GC-MS (selective-ion mode) detection and calculation of the relative intensities of the respective molecular ions selected over the fully resolved GC peaks. Corrections for the exact adamantane/adamantane-*d*₁₆ ratio used, as determined by GC-MS, were applied.

The intramolecular deuterium KIE was determined on adamantane-1,3-*d*₂ (deuterium enrichment: 97.7(1) %), synthesized from 1,3-dibromoadamantane according to a literature procedure.²⁹ The reaction (three trials) was performed under Ar and O₂ (4%) in N₂ in a manner similar to that described for the evaluation of the intermolecular KIE. KIE values for 1-adamantanol were calculated from the ratio of 1-adamantanol-*d*₂ over 1-adamantanol-*d*₁ determined by GC-MS evaluation of the relative areas corresponding to the respective molecular ions selected over the entire GC peak (unresolved for the two 1-adamantanols). Corrections were applied to the mass peak intensity of 1-adamantanol-*d*₂ (154) due to contribution from the masses of naturally abundant ¹³C and ²H isotopes in 1-adamantanol-*d*₁ (153). An isotopic purity correction for the incompletely deuterated substrate (that is, due to contamination of adamantane-1,3-*d*₂ by adamantane-1-*d*₁) was implemented following a published analysis.²⁹

X-ray Structure Determinations. Crystallographic data for compounds **3**, **5-7**, and **9-11** for which structures were determined are included only as Supporting Information. Single crystals were picked from the crystallization vessel (coated with Paratone-N oil if necessary due to air-sensitivity or desolvation), mounted on a glass fiber using grease, and transferred to a Siemens (Bruker) SMART CCD (charge coupled device) based diffractometer equipped with an LT-2 low-temperature apparatus operating at 213 K. Data were measured using omega scans of 0.3° per frame for 30 s (10 s for **5**; 60 s for **6** and **11**), such that a hemisphere was collected. A total of 1271 frames (1400 for **9**) were collected with a maximum resolution of 0.75 Å (0.85 Å for **5**, **9** and **10**). The first 50 frames were recollected at the end of data collection to monitor for decay. Cell parameters were retrieved using SMART software³⁰ and refined using the SAINT software³¹ which corrects for Lp and decay. Absorption corrections were applied using SADABS³² supplied by George Sheldrick. The structures are solved by the direct method using the SHELXS-97³³ program and refined by least-squares method on F², SHELXL-97,³⁴ incorporated in SHELXTL-PC V 5.10.³⁵

The structures were solved in the space groups specified in tables deposited as Supporting Information by analysis of systematic absences.

(29) Sorokin, A.; Robert, A.; Meunier, B. *J. Am. Chem. Soc.* **1993**, *115*, 7293–7299.

(30) SMART V 5.050 (NT) *Software for the CCD Detector System*; Bruker Analytical X-ray Systems: Madison, WI, 1998.

(31) SAINT V 5.01 (NT) *Software for the CCD Detector System*; Bruker Analytical X-ray Systems: Madison, WI, 1998.

(32) SADABS *Program for Absorption Corrections Using Siemens CCD Based on the Method of Robert Blessing*; Blessing, R. H. *Acta Crystallogr.* **1995**, *A51*, 33–38.

All non-hydrogen atoms are refined anisotropically. Hydrogens were located by difference Fourier maps and refined isotropically. For **5**, **7**, and **11** hydrogens were calculated by geometrical methods and refined as a riding model. Water-molecule hydrogens in **7** were placed to accommodate hydrogen bonding. The solvent molecule of pyridine in **10** was modeled for disorder over the 2-fold axis. The crystals used for the diffraction studies showed no decomposition during data collection. All ORTEP drawings deposited as Supporting Information are done at 50% probability ellipsoids.

Other Physical Measurements. ¹H NMR spectra were recorded on JEOL GSX-270 and Varian XL-400 NMR spectrometers. The isotropically shifted peaks for the iron-containing compounds were assigned when possible based on chemical shift, integration, and selective deuteration. FT-IR spectra were obtained on a Perkin-Elmer 1800 spectrometer. UV-vis spectra were obtained on a Hewlett-Packard 8452A diode array spectrometer, equipped with an Oxford DN1704 cryostat and ITC4 temperature controller for low-temperature measurements. Electrospray ionization (ESI) mass spectra were recorded using a Platform II MS (Micromass Instruments, Danvers, MA). Samples were introduced from solutions specified in the text at a flow rate of 5 μL/min from a syringe pump (Harvard Apparatus). The electrospray probe capillary was maintained at a potential of 3.0 kV, and the orifice to skimmer potential (“cone voltage”) was varied from 15 to 30 V. Spectra were collected in the multichannel acquisition mode. EI and CI mass spectra were obtained on a Finnigan MAT-90 mass spectrometer. Fast atom bombardment (FAB) mass spectra were measured on a Kratos MS instrument. X-band ESR spectra were recorded on a Varian E9 spectrometer located at the Chemistry Department of Harvard University, employing an Oxford ESR-10 liquid-helium cryostat. Microanalyses were done by H. Kolbe, Mikroanalytisches Laboratorium, Mülheim an der Ruhr, Germany, and by Quantitative Technologies Inc., Whitehouse, NJ.

Results and Discussion

Synthesis and Characterization of Ferrous Picolinate Species. We initiate our investigation by summarizing the pertinent features and interconversion chemistry of ferrous and ferric (vide infra) picolinate species employed as oxidation reagents in the present study. Some of these precursors have been previously used in Gif and “oxygenated Fenton” chemistry, but have remained ill-defined. Stoichiometric transformations of the appropriate ferrous picolinate sites in pyridine suggest that these precursors are not suitable to mediate Gif oxygenations supported by O₂/Zn. On the other hand, ferric picolinate species are readily transformed to their ferrous congeners upon exposure to a small excess of H₂O₂. Thus, the oxygenation chemistry detailed in subsequent sections is most likely associated with oxidants produced by Fe^{II}/H₂O₂ combinations, irrespective of whether ferrous or ferric species are used as catalyst precursors.

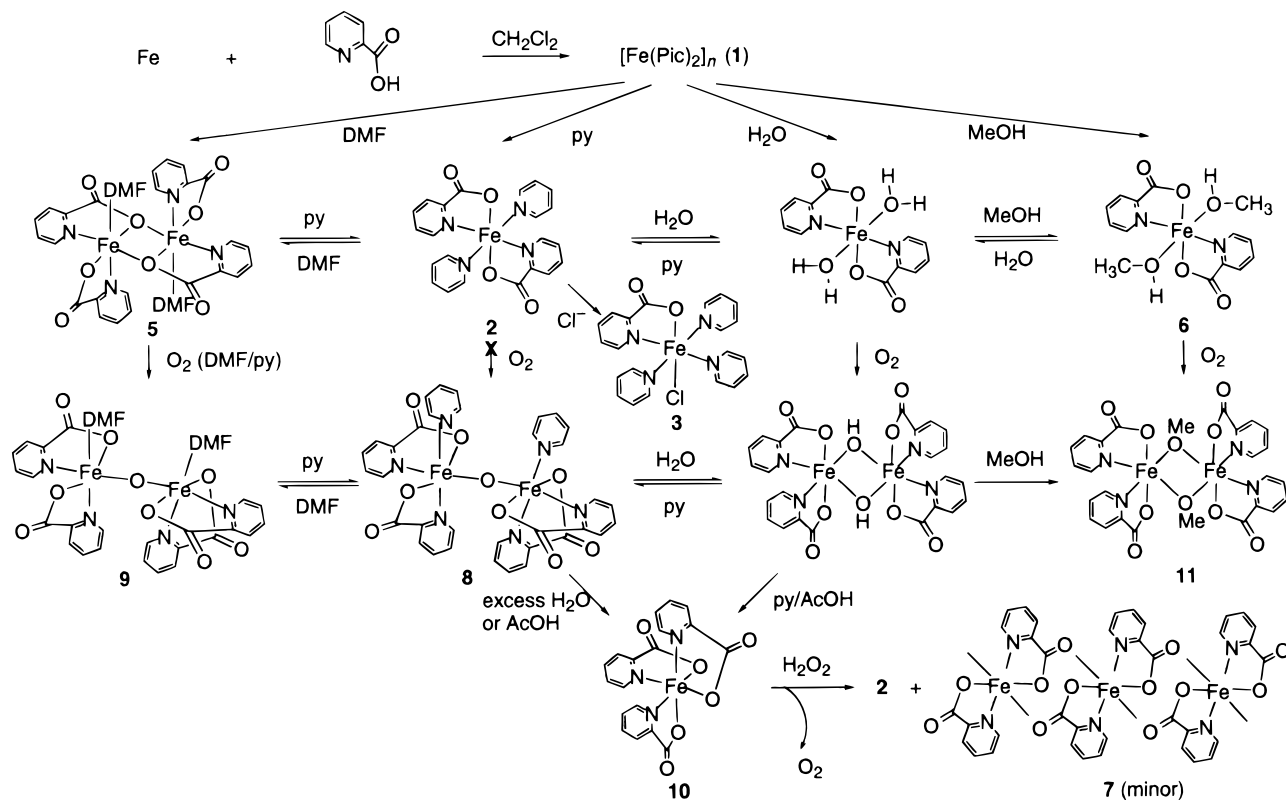
Scheme 2 summarizes the structural features and interconversion chemistry of key iron picolinate species under a variety of conditions. Detailed structural evidence has been deposited as Supporting Information. [Fe^{II}(Pic)₂]_n (**1**) precipitates as a red powder upon stirring metallic Fe and PicH (2 equiv) in CH₂Cl₂ under a dinitrogen atmosphere. Polymeric **1** dissociates to discrete mononuclear and/or dinuclear species in a variety of solvents. In pyridine, Gif's special solvent, **1** dissolves to afford orange-red crystals of analytically pure [Fe^{II}(Pic)₂(py)₂] (**2**). Compound **2**, which has not been amenable to X-ray analysis, is assigned as a mononuclear structure on the basis of micro-

(33) Sheldrick, G. M. *SHELXS-97 Program for the Solution of Crystal Structure*; University of Göttingen: Göttingen, Germany, 1997.

(34) Sheldrick, G. M. *SHELXL-97 Program for the Refinement of Crystal Structure*; University of Göttingen: Göttingen, Germany, 1997.

(35) SHELXTL 5.10 (PC-Version) *Program Library for Structure Solution and Molecular Graphics*; Bruker Analytical X-ray Systems: Madison, WI, 1998.

Scheme 2



analytical and positive-ion electrospray MS data obtained from pyridine solutions of **2** ($m/z = 459$ [M + H]⁺). ¹H NMR data in CD₂Cl₂ and pyridine-*d*₅ suggest that the solid-state structure is retained in solutions. In an attempt to crystallize **2** from a mixture of pyridine and CH₂Cl₂ (1:1 v/v) red crystals of [Fe^{II}(Pic)(py)₃Cl] (**3**) were deposited (see Supporting Information for solid-state structure) along with colorless crystals of [C₅H₅N-CH₂-NC₅H₅]₂Cl₂. The latter compound, which remarkably precipitates even from mixtures of routinely purified pyridine and CH₂Cl₂ (1:1 v/v) alone, is presumably the source of chloride found in **3**.

Polymeric **1** dissociates in 4-*tert*-butylpyridine to afford carmine-red [Fe^{II}₂(Pic)₄(4-*t*-Bupy)₂] (**4**), albeit in microcrystals not suitable for X-ray analysis. Based on microanalytical data, the compound is formulated as a dimeric structure similar to that encountered in the case of the DMF adduct **5** (see below). ¹H NMR spectra in CD₂Cl₂ support this assignment and extend it to solution structures by providing an integrated ratio of Pic/4-*t*-Bupy equal to 2:1. In DMF, compound **1** dissolves to yield red crystals of [Fe^{II}₂(Pic)₄(DMF)₂] (**5**). The same compound can also be obtained in quantitative yields by dissolving **2** in DMF. The solid-state structure of **5** (see Supporting Information) consists of a dimeric molecule featuring a pair of ferrous sites bridged via two carboxylato oxygens derived from two Pic moieties. The dinuclear structure of **5** is apparently retained in dimethylformamide, as indicated by ESI-MS data ($m/z = 746$ [M]⁺).

Hints to the structure of the pyridine adduct **2** are offered by the geometric features of [Fe^{II}(Pic)₂(MeOH)₂] (**6**) and the known compound [Fe^{II}(Pic)₂(H₂O)₂]·2H₂O.³⁶ The methanol adduct **6**, which has been crystallographically investigated (see Supporting Information), is obtained as orange crystals from solutions of **1** or **2** in MeOH. The ¹H NMR spectrum of **6** in CD₂Cl₂ suggests

that the mononuclear structure persists in solution. A similar structure has been reported³⁶ for the water adduct [Fe^{II}(Pic)₂(H₂O)₂]·2H₂O, which in the present study is obtained by dissolving polymeric **1** in water, but also via all other Fe(II) complexes noted above. Interestingly, a light-blue compound of stoichiometry [Fe^{II}(Pic)₂]·2H₂O (**7**) has been isolated in low yields among the decomposition products of the reaction of [Fe(Pic)₃]·0.5py (**10**) with H₂O₂ (vide infra), and recrystallized from wet methanolic solutions. The structure of **7** (see Supporting Information) reveals layers composed of discrete planar centrosymmetric [Fe(Pic)₂] units featuring weak intermolecular interactions (Fe–O = 2.734 Å) via adjacent carbonyl moieties along the axial coordination vector. Surprisingly, compound **7**, dissolved in methanol or water, retains its light blue color and does not convert to **6** or [Fe^{II}(Pic)₂(H₂O)₂]. It is also worthwhile noting that the solvated ferrous species **2–6** interconvert by virtue of facile solvent exchange.

Synthesis and Characterization of Ferric Picolinate Species. Compound [Fe^{III}(Pic)₂(py)₂] (**2**) is moderately stable upon exposure to dioxygen. This behavior may explain why catalytic oxygenation of hydrocarbons mediated by Fe(II)-picolinate species in pyridine or py/AcOH would not operate under O₂/Zn but require H₂O₂ instead. Compound [Fe^{III}₂O(Pic)₄(py)₂] (**8**) can be synthesized indirectly upon dissolving [Fe^{III}O(Pic)₄(DMF)₂] (**9**) in pyridine. Unfortunately, we have been unable to obtain crystals of light-brown **8** suitable for X-ray analysis. Microanalytical, IR ($\nu_{\text{Fe-O-Fe(asy)}} = 856$ cm⁻¹), ¹H NMR, and ESI-MS data ($m/z = 696$ [M + H - py]⁺) strongly support the assignment of **8** as a diferric μ -oxo structure similar to that encountered in the solid-state structure of brown-red **9** (see Supporting Information). Generation of **9**³⁷ is possible via compound **2**, which, when dissolved in DMF, transforms to **5** and becomes sensitive upon exposure to dioxygen, most likely due to facile replacement of DMF. However, stoichiometric

(36) Shova, S. G.; Brashovyanu, N. V.; Turte, K. I.; Mazus, M. D. *Russ. J. Coord. Chem.* **1996**, *22*, 438–443.

amounts of pyridine in solutions of **5** in DMF are necessary to achieve formation of **9**, otherwise the oxo bridge of **9** is not retained and only $[\text{Fe}(\text{Pic})_3]\cdot\text{DMF}$ is obtained. Further verification of the structure of **9** is provided by the detection of the $\nu_{\text{Fe-O}-\text{Fe}(\text{asym})}$ stretching band in the solid state (867 cm^{-1}) in accord with values reported³⁸ for similar μ -oxo diferric compounds. ¹H NMR spectra of **9** in CD_2Cl_2 and ESI-MS data from DMF solutions ($m/z = 690 [\text{M} + \text{H} - \text{DMF}]^+$) indicate that this structure is also retained in solution.

In the presence of protic solvents such as excess water or CH_3COOH , the oxo bridge of **8** has also proven to be fragile, leading to generation of $[\text{Fe}(\text{Pic})_3]\cdot 0.5\text{py}$ (**10**) in pyridine. Importantly, exposure of **10** to 2 equiv of H_2O_2 in pyridine generates purple colored solutions at low temperatures ($< -20\text{ }^\circ\text{C}$) which decompose rapidly at higher temperatures ($> 5\text{ }^\circ\text{C}$) to reform, upon evolution of O_2 , the reduced $[\text{Fe}^{\text{II}}(\text{Pic})_2(\text{py})_2]$ (**2**) and trace amounts of $[\text{Fe}^{\text{II}}(\text{Pic})_2]\cdot 2\text{H}_2\text{O}$ (**7**). The nature of the intermediate purple solution is currently under consideration.

Finally, the ferrous species $[\text{Fe}^{\text{II}}(\text{Pic})_2(\text{MeOH})_2]$ (**6**) and $[\text{Fe}^{\text{II}}(\text{Pic})_2(\text{H}_2\text{O})_2]\cdot 2\text{H}_2\text{O}$ ³⁶ are oxidized by dioxygen to yield $[\text{Fe}^{\text{III}}_2(\mu\text{-OMe})_2(\text{Pic})_4]$ (**11**) and $[\text{Fe}^{\text{III}}_2(\mu\text{-OH})_2(\text{Pic})_4]$ ³⁹ in methanol and water, respectively. The pale-yellow hydroxo-bridged ferric compound has been previously reported³⁹ and proven difficult to crystallize, as it precipitates rapidly from water and transforms to other species in a variety of solvents. In pyridine, $[\text{Fe}^{\text{III}}_2(\mu\text{-OH})_2(\text{Pic})_4]$ reverts to $[\text{Fe}^{\text{III}}_2\text{O}(\text{Pic})_4(\text{py})_2]$ (**8**), while in py/AcOH affords $[\text{Fe}(\text{Pic})_3]\cdot 0.5\text{py}$ (**10**). The slightly more acidic methanol converts the hydroxy-bridged $[\text{Fe}^{\text{III}}_2(\mu\text{-OH})_2(\text{Pic})_4]$ to the corresponding methoxy-bridged species **11** (see Supporting Information for solid-state structure).

Catalytic Oxidation of Adamantane Mediated by Fe(II) Reagents. Table 1 summarizes product profiles for the oxygenation of adamantane (5 mmol) by H_2O_2 (2 mmol; added by syringe pump in the course of the reaction) catalyzed by the ferrous compound $[\text{Fe}^{\text{II}}(\text{Pic})_2(\text{py})_2]$ (**2**) (0.2 mmol). The oxygenation reactions are performed in a solvent matrix composed of pyridine (30.0 mL) and carboxylic acid(s), namely AcOH (3.0 mL) and/or PicH (50 mg, 0.40 mmol, or 2 g, 16.3 mmol). Occasionally, excess Zn (1.3 g, 20.0 mmol) is added to the reaction mixture as a sacrificial reducing agent. The catalytic reactions are conducted under inert atmosphere (N_2 , Ar) or variable partial pressures of dioxygen (O_2 (4%) in N_2 , air, O_2 (100%)).

Inspection of the product profile obtained from the oxygenation of adamantane reveals activation of both tertiary and secondary positions. The products detected are divided into two categories: oxo products (1-adamantanol (1-ol), 2-adamantanol (2-ol), adamantanone (2-one)) and adamantyl-pyridines (2-(1-Ad)-py, 4-(1-Ad)-py, 2-(2-Ad)-py, 4-(2-Ad)-py). In addition, products of pyridine oxidation, namely hydroxypyridines and bipyridines, are obtained. These products have been previously quantified in Gif^{IV}-type oxygenation chemistry ($\text{Fe}_{\text{cat}}/\text{O}_2/\text{Zn}$);⁷ no attempts to account for products of pyridine oxidation have been made with the present systems.

Entry 1 (Table 1) reveals the most important finding in these series of adamantane oxidations. Under dinitrogen, not only *tert*-adamantylpyridines (2-(1-Ad)-py, 4-(1-Ad)-py) are obtained but

Table 1. Product Profile of Adamantane Oxidation by H_2O_2 Mediated by $[\text{Fe}(\text{Pic})_2(\text{py})_2]$ (**2**)

System	Products (mmol)							$3^\circ/2^\circ$
	OH	OH	OH					
1. N_2^a	0.008	0.044	0.121	0.142	0.135	0.091	0.041	2.88
2. O_2^a	0.270	0.052	0.175	0.006	0.010	nd	nd	3.78
3. O_2^a	0.070	0.014	0.175	0.082	0.082	0.009	0.010	3.38
4. N_2^b	nd	nd	0.023	0.160	0.169	0.082	0.111	4.57
5. Ar ^c	nd	nd	0.017	0.122	0.110	0.115	0.163	2.36
6. O_2^c	0.269	0.068	0.195	0.006	0.008	nd	nd	3.21
7. N_2^d	tr	tr	tr	0.064	0.055	0.054	0.081	2.64
8. O_2^d	0.145	0.036	0.110	nd	nd	nd	nd	2.86
9. Ar ^e	0.020	0.059	0.118	0.044	0.084	0.007	0.021	2.17
10. O_2^e	0.216	0.073	0.200	0.029	0.057	nd	nd	3.32
11. N_2^f	0.040	0.020	0.010	na	na	na	na	4.00
12. O_2^f	0.113	0.054	0.040	na	na	na	na	3.61

^a General conditions, unless otherwise noted: 0.2 mmol **2**; 5 mmol AdH; 2 mmol H_2O_2 (added by syringe pump over 6 hours at RT); py/AcOH (30/3 mL). nd = not detected. tr = trace amount. na = not applicable. ^b 20 mmol of Zn dust added. ^c 0.4 mmol of PicH added. ^d 16.3 mmol of PicH added; AcOH omitted. ^e 0.4 mmol of PicH added; AcOH omitted. ^f Py omitted; 30 mL of CH_3CN added.

also *sec*-adamantylpyridines (2-(2-Ad)-py, 4-(2-Ad)-py) are detected in comparable yields. These coupling products dominate the product profile especially with regards to the activation of the *tert*-adamantyl positions (the ratio of pyridine-coupled versus oxo products is 34.6) and to a lesser extent of the *sec*-adamantyl sites (the corresponding ratio is 0.8). Other important mechanistic indicators are (i) the prominence of 2-one formation over 2-ol (2-one/2-ol ≈ 3), which is not due to overoxidation of 2-ol to 2-one, and thus precludes simple "oxenoid" insertion into C-H bonds; and (ii) the overall selectivity for the activation of tertiary versus secondary positions on a per hydrogen basis ($3^\circ/2^\circ = 2.88$), which suggests that the active oxidant involved displays modest selectivity. Similarly low *tert/sec* selectivity values are reported for H_2O_2 ⁴⁰ or O_2/Zn -dependent⁴¹ oxidations of adamantane mediated by other oxygenation systems. The *t*-BuOOH supported systems⁴² provide a value $3^\circ/2^\circ \approx 10$ in accord with radical hydrogen-abstraction from adamantane by *t*-BuO[•].³ These values need to be contrasted with values of 11–48 for oxidations of adamantane by P-450/PhIO biomimetic systems,⁴³ although a surprisingly low value ($3^\circ/2^\circ = 3$) has been reported⁴⁴ for adamantane oxidation by sMMO.

The detection of adamantylpyridines is *prima facie* indication of the involvement of adamantyl radicals, since alkyl radicals are known to attack protonated pyridine at positions 2- and 4-,

(37) A compound assigned to $[\text{Fe}_2\text{O}(\text{Pic})_4]$ has been previously synthesized from DMF solutions. The reported compound is most likely identical to **9**: (a) Sheu, C.; Richert, S. A.; Cofré, P.; Ross, B., Jr.; Sobkowiak, A.; Sawyer, D. T.; Kanofsky, J. R. *J. Am. Chem. Soc.* **1990**, *112*, 1936–1942. (b) Cofré, P.; Richert, S. A.; Sobkowiak, A.; Sawyer, D. T. *Inorg. Chem.* **1990**, *29*, 2645–2651.

(38) Kurtz, D. M., Jr. *Chem. Rev.* **1990**, *90*, 585–606.

(39) Schugar, H. J.; Rossman, G. R.; Gray, H. B. *J. Am. Chem. Soc.* **1969**, *91*, 4564–4566.

(40) (a) Fish, R. H.; Konings, M. S.; Oberhausen, K. J.; Fong, R. H.; Yu, W. M.; Christou, G.; Vincent, J. B.; Coggin, D. K.; Buchanan, R. M. *Inorg. Chem.* **1991**, *30*, 3002–3006. (b) Vincent, J. B.; Huffman, J. C.; Christou, G.; Li, Q.; Nanny, M. A.; Hendrickson, D. N.; Fong, R. H.; Fish, R. H. *J. Am. Chem. Soc.* **1988**, *110*, 6898–6900.

(41) (a) Kitajima, N.; Ito, M.; Fukui, H.; Moro-oka, Y. *J. Chem. Soc., Chem. Commun.* **1991**, 102–104. (b) Kitajima, N.; Fukui, H.; Moro-oka, Y. *J. Chem. Soc., Chem. Commun.* **1988**, 485–486.

(42) (a) Kojima, T.; Leising, R. A.; Yan, S.; Que, L., Jr. *J. Am. Chem. Soc.* **1993**, *115*, 11328–11335. (b) Ménage, S.; Vincent, J. M.; Lambeaux, C.; Chottard, G.; Grand, A.; Fontecave, M. *Inorg. Chem.* **1993**, *32*, 4766–4773.

(43) Groves, J. T.; Nemo, T. E. *J. Am. Chem. Soc.* **1983**, *105*, 6243–6248.

(44) Green, J.; Dalton, H. *J. Biol. Chem.* **1989**, *264*, 17698–17703.

via pathways extensively studied by Minisci.⁴⁵ This is further reinforced by the results of oxidation experiments under dioxygen (entry 2), which mark a substantial deviation from the product distribution observed under N₂ (entry 1). Indeed, *sec*-adamantylpyridines have now disappeared in favor of 2-one and to a lesser extent 2-ol, and *tert*-adamantylpyridines have been diminished to low yields in favor of the major oxygenation product 1-ol. Interestingly, the *tert/sec* selectivity is enhanced ($3^\circ/2^\circ = 3.78$), suggesting partial interference of a more selective active oxidant. At low partial pressure of dioxygen (4% of O₂ in N₂ (entry 3)), an intermediate product profile, between those observed in pure N₂ and O₂, is obtained. The conditions under 4% O₂ provide good yields of all products for control experiments purported to scrutinize whether the entire product distribution is due to partitioning of *tert*- and *sec*-adamantyl radicals between dioxygen and protonated pyridine (vide infra). In the presence of excess zinc under N₂, added with the intention of rapidly reducing any Fe(III) formed to Fe(II) and thus avoiding byproducts of Fe(III)/H₂O₂ dependent cycles (including dioxygen), the product profile (entry 4) shifts almost exclusively toward formation of *tert*- and *sec*-adamantylpyridines, as expected, but surprisingly the *tert/sec* selectivity ($3^\circ/2^\circ = 4.57$) is one of the highest observed in the present study. Addition of small amounts of picolinic acid (2 equiv over **2**) to the reaction mixture (py/AcOH) shows no ligand-enhancing effect on the product profile of oxygenations conducted under argon (entry 5) or dioxygen (entry 6), with the exception that adamantylpyridines are prominently represented under argon, probably due to the effectiveness of argon in removing adventitious dioxygen. Replacement of acetic acid by equimolar amounts of picolinic acid diminishes the overall yield of products (entries 7 and 8) to almost half. In contrast, catalytic amounts of picolinic acid (2 equiv over **2**) in the absence of AcOH, are as effective as AcOH (especially under O₂ (entry 10)) in bringing about oxidation of adamantane, although under argon (entry 9) the amounts of adamantylpyridines are relatively suppressed in favor of the oxo products (*tert* Ad-py/Ad(O) = 6.4, *sec* Ad-py/Ad(O) = 0.16), most likely owing to the limited protonation of pyridine.⁴⁵ Finally, attempts to replace py/AcOH by CH₃CN/AcOH (10:1 v/v) yielded low amounts of oxo products (entries 11 and 12). The alcohol 1-ol is the major product followed by 2-ol, which exceeds the amount of 2-one observed. The preponderance of 2-ol over 2-one may not necessarily signify change in mechanism, as it could possibly reflect different processing of *sec*-adamantyl radicals in CH₃CN/AcOH (usual H-atom abstraction)¹⁷ versus py/AcOH (C- to O-atom 1,2-H migration (Scheme 1)).

Catalytic Oxidation of Adamantane Mediated by Fe(III) Reagents. Collected in Table 2 are product profiles obtained from H₂O₂-dependent oxidations of adamantane mediated by a number of Fe(III) reagents ([Fe(Pic)₃]·0.5py (**10**), [Fe^{III}₂O(Pic)₄-(py)₂] (**8**), [Fe^{III}₂(μ-OH)₂(Pic)₄], as well as FeCl₃). Most data derive from oxygenations involving [Fe(Pic)₃]·0.5py (**10**), since this reagent is readily generated by other Fe(III) picolinic species (such as **8** or [Fe^{III}₂(μ-OH)₂(Pic)₄]) in py/AcOH. Conditions employed in catalytic oxygenations by Fe(III)/H₂O₂ reagents are similar to those used with Fe(II)/H₂O₂ combinations, thus permitting direct comparison of the two systems.

The product distribution obtained from the oxidation of adamantane (5 mmol) by H₂O₂ (2 mmol) in py/AcOH (10:1 v/v) in the presence of [Fe(Pic)₃]·0.5py (**10**, 0.2 mmol) under N₂ (Table 2, entry 1) exhibits similar features to those previously

Table 2. Product Profile of Adamantane Oxidation by H₂O₂ Mediated by [Fe(Pic)₃]·0.5py (**10**), [Fe₂O(Pic)₄-(py)₂] (**8**), [Fe₂(μ-OH)₂(Pic)₄], and FeCl₃

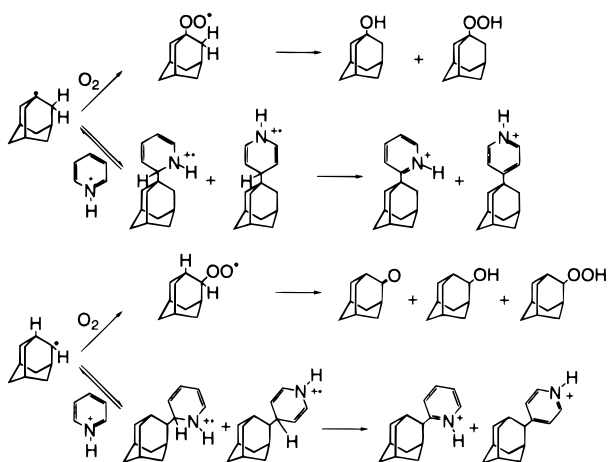
System	Products (mmol)							3°/2°
								
1. N ₂ ^a	0.031	0.046	0.134	0.083	0.120	0.034	0.052	2.64
2. O ₂ ^a	0.255	0.043	0.186	0.006	0.013	nd	nd	3.61
3. O ₂ ^a (4%)	0.063	0.024	0.171	0.071	0.074	0.007	0.010	2.94
4. N ₂ ^b	0.011	0.037	0.119	0.086	0.143	0.045	0.078	2.58
5. O ₂ ^b	0.250	0.042	0.185	0.006	0.013	nd	nd	3.56
6. Ar ^c	0.020	0.074	0.139	0.062	0.102	0.015	0.026	2.17
7. O ₂ ^c	0.259	0.070	0.182	0.004	0.008	nd	nd	3.23
8. N ₂ ^d	0.026	0.033	0.094	0.064	0.089	0.028	0.036	2.81
9. O ₂ ^d	0.205	0.034	0.105	0.005	0.005	nd	nd	3.56
10. Ar ^e	0.039	0.083	0.116	0.053	0.055	tr	tr	2.22
11. O ₂ ^e	0.056	0.048	0.184	0.093	0.107	tr	tr	3.31
12. N ₂ ^f	0.009	nd	0.106	0.107	0.075	nd	nd	3.16
	0.010 ^g	0.085 ^h						

^a General conditions, unless otherwise noted: 0.2 mmol **10**; 5 mmol AdH; 2 mmol H₂O₂ (added by syringe pump over 6 hours at RT); py/AcOH (30/3 mL). nd = not detected. ^b 0.2 mmol of PicH added. ^c AcOH omitted. ^d **10** replaced by **8**. ^e **10** replaced by [Fe₂(μ-OH)₂(Pic)₄]. ^f **10** replaced by FeCl₃. ^g 1-Cl-Ad. ^h 2-Cl-Ad.

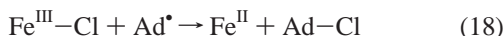
observed in oxygenations mediated by [Fe^{II}(Pic)₂(py)₂] (**2**), chief among which is the detection of both *tert*- and *sec*-adamantylpyridines. However, by comparison to the corresponding oxo products, the amount of adamantylpyridines is suppressed (*tert* Ad-py/Ad(O) = 6.55, *sec* Ad-py/Ad(O) = 0.48), probably due to internally produced dioxygen (and/or superoxide). Under pure O₂ or 4% O₂ (in N₂) (entries 2, 3), the product profile shifts gradually in favor of the oxo products, in a manner paralleling that observed with the Fe(II) reagent, including the tendency for the *tert/sec* selectivity to increase with increasing amounts of dioxygen ($3^\circ/2^\circ = 2.64$ (N₂), 3.61 (O₂)). Addition of one more equivalent of PicH over iron in the reaction mixture has no effect on product distribution (entries 4, 5). However, if this small excess of PicH is present in solution in the absence of any AcOH, then, in analogy to results obtained with [Fe^{II}(Pic)₂(py)₂] (**2**), the amount of adamantylpyridines is relatively diminished in favor of oxo products (entries 6, 7). Adamantane oxygenations mediated by [Fe^{III}₂O(Pic)₄(py)₂] (**8**) show similar product profiles (entries 8, 9) to those obtained with **10**, but [Fe^{III}₂(μ-OH)₂(Pic)₄] (entries 10, 11) affords only traces of *sec*-adamantylpyridines under Ar. It is unlikely that the near absence of these products signifies any change in mechanism. The low *tert/sec* selectivity ($3^\circ/2^\circ = 2.22$) observed in these experiments minimizes the possibility that internally produced fluxes of O₂ may have affected the product profile. However, the unusually high amounts of 2-ol obtained relative to 2-one suggest that Fe^{III}-OH units may efficiently scavenge *sec*-adamantyl radicals to generate 2-ol. A similar situation is encountered with a reagent commonly used by Barton in mechanistic studies,³ namely FeCl₃ in py/AcOH. Indeed, oxygenation of adamantane by this reagent does not afford any detectable amounts of *sec*-adamantylpyridines under inert atmosphere (entry 12). However, the presence of 2-chloro-adamantane, formed at much higher quantities than 1-chloro-adamantane, fully compensates for the lack of *sec*-adamantylpyridine products. Chlorine-atom abstraction by adamantyl

(45) Minisci, F.; Vismara, E.; Fontana, F. *Heterocycles* **1989**, 28, 489–519.

Scheme 3



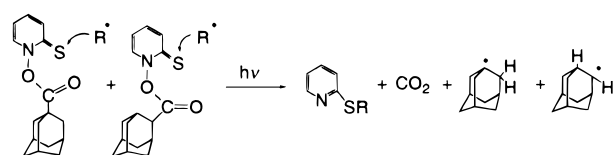
radicals from FeCl_3 derivatives (eq 18) is most likely the source of chloroadamantanes.



Control Experiments with Authentic Adamantyl Radicals.

To secure that the product profiles of adamantane oxidations mediated by $[\text{Fe}^{\text{II}}(\text{Pic})_2(\text{py})_2]$ (**2**) and $[\text{Fe}(\text{Pic})_3] \cdot 0.5\text{py}$ (**10**) are uniquely determined by competition between dioxygen and protonated pyridine for capturing *tert*- and *sec*-adamantyl radicals, we revisited an early control experiment²⁶ that has been central to Barton's argument¹ in support of a non-radical mechanism for the activation of *sec*-adamantyl sites in Gif chemistry. Assuming that authentic *tert*- and *sec*-adamantyl radicals (Scheme 3) are generated in py/AcOH (10/1 v/v) under 4% O_2 in N_2 (for instance, via photolysis of Barton's PTOC esters²⁶), their fate will be determined by competitive partitioning between dioxygen trapping and addition to pyridinium cation. Dioxygen trapping is expected²² to be diffusion controlled for both types of radicals to yield the corresponding adamantlyperoxy radicals, which are the precursors of all oxo products. On the other hand, the reversible addition of *tert*- and *sec*-adamantyl radicals at positions 2- and 4- of protonated pyridine to generate the corresponding adamantlypyridinium radicals has been anticipated²² to proceed at different rates for the two radicals. Indeed, recent measurements by Minisci⁴⁶ have provided rate constants of $2.2 \times 10^6 \text{ M}^{-1} \text{ s}^{-1}$ and $1.3 \times 10^4 \text{ M}^{-1} \text{ s}^{-1}$ for the addition of *tert*- and *sec*-adamantyl radicals to pyridinium cation, respectively. The origin of the difference, by 2 orders of magnitude, between the two rate constants is traced⁴⁶ to the substantial charge-transfer character of the transition state, which favors the more nucleophilic *tert*-adamantyl radical. The so obtained adamantlypyridinium radicals are highly reducing and readily rearomatize to the final adamantlypyridine products. Barton's control experiments²⁶ with authentic adamantyl radicals showed that at 4% O_2 in N_2 the ratio of oxygen-trapped over pyridine-coupled adamantyl products is 0.74 for the tertiary positions and 4.3 for the secondary sites, reflecting the different rates for *tert*- and *sec*-adamantyl radical addition to pyridinium. In contrast, a typical oxidation of adamantane by a Gif^{IV}-type reagent ($\text{FeCl}_2/\text{Zn}/\text{O}_2$ (4%)) afforded²⁶ a corresponding ratio of 0.03 for the tertiary positions and 94 for the secondary sites. While the preponderance of *tert*-adamantlypyridines in Gif chemistry was interpreted²⁶ as solid evidence for the presence of *tert*-adamantyl radicals (and the

Scheme 4



numerical discrepancy with respect to the control experiment was explained as preferential addition of *tert*-adamantyl radicals to pyridine coordinated to iron), the near absence of *sec*-adamantlypyridines was taken as evidence for the lack of diffusively free *sec*-adamantyl radicals in Gif chemistry. Minisci has recently reinterpreted⁴⁶ the latter result by hypothesizing that the Gif conditions do not favor the irreversible rearomatization process, thus, by virtue of the more reversible *sec*-adamantyl-radical addition to pyridinium, dioxygen is permitted to compete most effectively by trapping *sec*-adamantyl radicals. However, the same argument should also predict that by comparison to the control experiment, *tert*-adamantyl oxo products ought to be somewhat more enhanced under Gif conditions; the reverse is actually realized in Barton's experiments²⁶ by a large margin (see below for further discussion).

In the present study, authentic *tert*- and *sec*-adamantyl radicals are generated via photolysis of the corresponding *N*-adamantylcarboxylpyridine-2-thione derivatives (0.115 mmol of each) in py/AcOH (10:1 mL) under a stream of 4% O_2 in N_2 (Scheme 4). The so formed *tert*- and *sec*-adamantyl radicals are competitively captured by three traps present in solution: dioxygen, protonated pyridine, and the 2-pyridylthiyl moiety of Barton's esters. In contrast to Barton's control experiments which are conducted in the absence of metal, reagents $[\text{Fe}^{\text{II}}(\text{Pic})_2(\text{py})_2]$ (**2**) or $[\text{Fe}(\text{Pic})_3] \cdot 0.5\text{py}$ (**10**) are added to py/AcOH at concentrations comparable to those employed in Gif oxygenations. This is necessary in order to better mimic the conditions of the Gif experiment, especially since metal ions can be readily involved in redox reactions with alkyl radicals and thus influence the result of the competition kinetics. Importantly, neither reagent generates Gif-type oxygenation systems in the presence of O_2 and a reducing agent (they are strictly H_2O_2 -dependent in their oxygenation activity), so potential complications due to interference of oxygen-centered radicals such as $\text{HO}^{\bullet}/\text{HOO}^{\bullet}$ are minimized.

Collected in Table 3 are numerical results of the quantification (by GC) of oxygenated and pyridine-coupled adamantyl products generated in the control experiments noted above, in the presence of $[\text{Fe}^{\text{II}}(\text{Pic})_2(\text{py})_2]$ (**2**) and $[\text{Fe}(\text{Pic})_3] \cdot 0.5\text{py}$ (**10**). Mass balances are provided by AdS-py and AdCOOH (derived by hydrolysis of the precursor esters), both of which were not quantified as they do not alter the results of adamantyl radical partitioning between dioxygen and protonated pyridine. In the presence of **2** (entry 1), the calculated ratio of oxygen-trapped versus pyridine coupled *tert*-adamantyl radicals ($\text{tert Ad(O)}/\text{Ad-py}$) equals 0.37, whereas the corresponding ratio for the secondary position ($\text{sec Ad(O)}/\text{Ad-py}$) is 12.0. Similar results are obtained in the presence of **10** (entry 2), for which $\text{tert Ad(O)}/\text{Ad-py}$ is 0.44 and $\text{sec Ad(O)}/\text{Ad-py}$ equals 12.8. By comparison to Barton's results²⁶ derived from experiments in the absence of metals, the corresponding numerical values ($\text{tert Ad(O)}/\text{Ad-py} = 0.74$; $\text{sec Ad(O)}/\text{Ad-py} = 4.3$) are within the same order of magnitude, although the presence of the iron reagents tends to relatively enhance pyridine-trapped products in the case of *tert*-adamantyl radicals, and dioxygen-captured derivatives in the case of *sec*-adamantyl radicals. Another interesting observation is that 2-one is favored over 2-ol both

(46) Recupero, F.; Bravo, A.; Bjørsvik, H.-R.; Fontana, F.; Minisci, F.; Piredda, M. *J. Chem. Soc., Perkin Trans. 2* **1997**, 2399–2405.

Table 3. Partition of Authentic and Gif Produced *tert*- and *sec*-Adamantyl Radicals between Dioxigen, Protonated Pyridine and TEMPO

System	Products (mmol)								$3^\circ/2^\circ$	$\frac{\text{Ad(O)}}{\text{Ad-py}}$		$\frac{\text{Ad-TEMPO}}{\text{Ad(O)}}$	
										<i>tert</i>	<i>sec</i>	<i>tert</i>	<i>sec</i>
1. 2 /O ₂ (4%) ^a	0.014	0.003	0.045	0.018	0.020	0.002	0.002			0.37		12.0	
2. 10 /O ₂ (4%) ^a	0.014	0.004	0.047	0.014	0.018	0.002	0.002			0.44		12.8	
3. 2 /O ₂ (4%) ^b	0.070	0.014	0.175	0.082	0.082	0.009	0.010			3.38	0.43	10.0	
4. 10 /O ₂ (4%) ^b	0.063	0.024	0.171	0.071	0.074	0.007	0.010			2.94	0.43	11.5	
5. 2 /N ₂ ^c	0.032	nd	0.039	0.013	0.018	nd	nd	0.179	0.195	3.10		5.6	5.0
6. 2 /N ₂ ^d	0.050	nd	0.062	0.009	0.011	nd	nd	0.114	0.123	2.98		2.3	2.0
7. 2 /O ₂ ^c	0.164	nd	0.174	0.001	0.003	nd	nd	0.086	0.077	3.04		0.52	0.44
8. 2 /O ₂ ^e	0.140	nd	0.152	0.002	0.002	nd	nd	0.078	0.070			0.56	0.46
9. 10 /O ₂ ^c	0.148	nd	0.152	0.002	0.002	nd	nd	0.074	0.098	2.71		0.50	0.64
10. 10 /O ₂ ^e	0.145	nd	0.138	0.002	0.002	nd	nd	0.080	0.095			0.55	0.69

^a 9.2 μmol **2** or **10** as specified; 0.115 mmol of *N*-adamantyl-1-carboxylpyridine-2-thione and *N*-adamantyl-2-carboxylpyridine-2-thione each; $h\nu$ (ACE-Hanovia mercury lamp); py/AcOH (10/1 mL); 2 h. nd = not detected. ^b 0.20 mmol **2** or **10** as specified; 5.0 mmol AdH; 2.0 mmol H₂O₂ (added by syringe pump over 6 hours at RT); py/AcOH (30/3.0 mL). ^c 5.0 mmol of TEMPO added to solutions specified in (b). ^d 2.0 mmol of TEMPO added to (b). ^e 0.02 mmol **2** or **10** as specified; 0.250 mmol of *N*-adamantyl-1-carboxylpyridine-2-thione and *N*-adamantyl-2-carboxylpyridine-2-thione each; 0.50 mmol of TEMPO; $h\nu$ (ACE-Hanovia mercury lamp); py/AcOH (3.0/0.30 mL); 2 h.

in the absence of metal in Barton's experiments (although the presence of 2-Ad-OOH obscures the picture) and most prominently in the presence of iron reagents in the present study.

The product profiles provided by the corresponding Gif oxidations under 4% O₂ in N₂ afford calculated values of *tert* Ad(O)/Ad-py and *sec* Ad(O)/Ad-py equal to 0.43 and 10.0 in the presence of [Fe^{II}(Pic)₂(py)₂] (**2**) (entry 3) and 0.43 and 11.5 in the presence of [Fe(Pic)₃]·0.5py (**10**) (entry 4), respectively. These values are in much better agreement to those obtained via control experiments featuring genuine adamantyl radicals (entries 1, 2), by comparison to values (*tert* Ad(O)/Ad-py = 0.08; *sec* Ad(O)/Ad-py = 94) reported by Barton,²⁶ derived from Gif^{IV}-type (Fe(II)/O₂ (4%)/Zn) oxygenations of adamantane. The agreement is better between experiments featuring authentic adamantyl radicals and Gif oxygenations involving [Fe(Pic)₃]·0.5py (**10**), and less so for those dependent on [Fe^{II}(Pic)₂(py)₂] (**2**). However, in the latter case values of *tert* Ad(O)/Ad-py and *sec* Ad(O)/Ad-py obtained from several Gif oxygenations were varying within a wider range, namely from 0.3 to 0.5 for the tertiary sites and from 8 to 12 for the secondary positions.

TEMPO-trapped Adamantyl Radicals. To ascertain that diffusively free *tert*-adamantyl radicals and most importantly *sec*-adamantyl radicals are generated in H₂O₂-dependent Gif oxygenations mediated by [Fe^{II}(Pic)₂(py)₂] (**2**) and [Fe(Pic)₃]·0.5py (**10**) under high partial pressures of O₂, a radical trap superior to protonated pyridine was sought to compete with dioxigen. This is particularly important for those oxygenations in which adamantylpyridines (especially *sec*-adamantylpyridines) are formed in trace amounts under the reaction conditions employed (high partial pressures of oxygen and/or limited protonation of pyridine) and would thus obscure interpretation of competition experiments.

TEMPO (2,2,6,6-tetramethyl-1-piperidinyloxy) is a widely used trap of carbon-centered radicals.⁴⁷ Rate constants for the

reactions of alkyl radicals with TEMPO have been measured^{47a} to be $\sim 1 \times 10^9 \text{ M}^{-1} \text{ s}^{-1}$ in hydrocarbons (somewhat lower values are obtained for resonance-stabilized radicals) and about half this value in water. The rate constants are inversely related to the thermodynamic stability of the carbon-centered radicals, and are also affected by steric factors. TEMPO was used in the present study to assess the formation of *tert*-Ad-TEMPO and *sec*-Ad-TEMPO in the course of Gif-type oxygenation of adamantane. Fortunately, both Ad-TEMPO products are volatile and stable under GC conditions, so that they can be quantified along with the other products of adamantane oxidation.

Table 3 (entries 5–10) summarizes product profiles of adamantane oxidation in the presence of TEMPO under variable conditions. Adamantane (5 mmol, entry 5) is oxidized by H₂O₂ (2 mmol) in reactions mediated by [Fe^{II}(Pic)₂(py)₂] (**2**) (0.2 mmol) under N₂ in the presence of TEMPO (5 mmol, 0.15 M) to afford almost exclusively 1-Ad-TEMPO and 2-Ad-TEMPO in amounts exceeding by 5-fold those of the corresponding oxo products (present in low yields). Minor amounts of only *tert*-adamantylpyridines are also present, confirming the superiority of TEMPO as a radical trap. The *tert*/*sec* selectivity ($3^\circ/2^\circ = 3.10$) is typical of similar Gif oxidations noted above, thus TEMPO does not seem to have an effect on the generation of the active oxidant involved. However, parallel oxidation processes do occur, as 4-oxo-TEMPO is detected among the reaction products in low yields. Furthermore, a control experiment under identical conditions indicated that adamantane-2-ol is readily converted to adamantane-2-one in the presence of TEMPO (but only to a limited extent in the absence of TEMPO). The transformation is probably due to metal-dependent one-electron oxidation of TEMPO to the corresponding oxoammonium cation, which is known⁴⁸ to mediate oxidation of alcohol to aldehydes or ketones, albeit slowly for secondary alcohols.

The competition between dioxigen and TEMPO becomes evident at lower concentrations of TEMPO (0.06 M, entry 6), as the preponderance of Ad-TEMPOs versus oxo products is

(47) (a) Chateaufort, J.; Luszyk, J.; Ingold, K. U. *J. Org. Chem.* **1988**, *53*, 1629–1632. (b) Beckwith, A. L. J.; Bowry, V. W.; Moad, G. *J. Org. Chem.* **1988**, *53*, 1632–1641. (c) Bowry, V. W.; Luszyk, J.; Ingold, K. U. *J. Am. Chem. Soc.* **1989**, *111*, 1927–1928. (d) Bowry, V. W.; Luszyk, J.; Ingold, K. U. *Pure Appl. Chem.* **1990**, *62*, 213–216.

(48) (a) Semmelhack, M. F.; Schmid, C. R.; Cortés, D. A.; Chou, C. S. *J. Am. Chem. Soc.* **1984**, *106*, 3374–3376. (b) Semmelhack, M. F.; Chou, C. S.; Cortés, D. A.; *J. Am. Chem. Soc.* **1983**, *105*, 4492–4494.

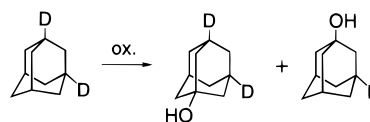
reduced to approximately 2-fold. The product profile under 4% O₂ in N₂ (not shown) is also very similar to that observed under N₂. It is only under pure dioxygen (entry 7) that the amounts of oxo products supersede those of the corresponding Ad-TEMPOs (*tert* Ad-TEMPO/Ad(O) = 0.52; *sec* Ad-TEMPO/Ad(O) = 0.44) in the presence of 0.15 M of TEMPO. Authentic *tert*- and *sec*-adamantyl radicals, generated by photolysis of the corresponding Barton's PTOC esters as previously indicated,⁴⁹ partition between dioxygen (100%) and TEMPO (0.15 M) in the presence of [Fe^{II}(Pic)₂(py)₂] (**2**) in a closely analogous manner (entry 8: *tert* Ad-TEMPO/Ad(O) = 0.56; *sec* Ad-TEMPO/Ad(O) = 0.46). Similar results have been obtained in oxidation experiments mediated by [Fe(Pic)₃]·0.5py (**10**). For example, under pure dioxygen (entry 9), the ratios of TEMPO-versus oxygen-trapped adamantyls (*tert* Ad-TEMPO/Ad(O) = 0.50; *sec* Ad-TEMPO/Ad(O) = 0.64) are analogous to those obtained in Gif oxygenations mediated by **2**. Once again, authentic adamantyl radicals generated via photolysis in the presence of **10**, partition between dioxygen (100%) and TEMPO (0.15 M) in an analogous fashion (entry 10: *tert* Ad-TEMPO/Ad(O) = 0.55; *sec* Ad-TEMPO/Ad(O) = 0.69).

The close correspondence between the aforementioned control experiments involving genuine adamantyl radicals and Gif oxygenations of adamantane mediated by [Fe^{II}(Pic)₂(py)₂] (**2**) or [Fe(Pic)₃]·0.5py (**10**) leads to the conclusion that the product profile of the oxygenation reactions is entirely dictated by the generation of *tert*- and *sec*-adamantyl radicals.

In Search of the Active Oxidant. (a) Kinetic Isotope Effect.

An intermolecular deuterium kinetic isotope effect (KIE) has been determined for the competitive Gif oxygenation of adamantane and adamantane-*d*₁₆ by **2** and **10** under dinitrogen. The KIE values obtained via GC-MS analysis of the product profile from three independent trials are as follows: 1-ol = 0.94(6) (**2**), 1.29(9) (**10**); 2-ol = 1.46(3) (**2**), 1.40(7) (**10**); 2-one = 1.88(4) (**2**), 1.99(14) (**10**); 2-(1-Ad)py = 0.81(3) (**2**), 0.86(5) (**10**); 4-(1-Ad)py = 1.41(4) (**2**), 1.39(2) (**10**); 2-(2-Ad)py = 1.64(15) (**2**), 1.51(8) (**10**); 4-(2-Ad)py = 1.38(5) (**2**), 1.36(3) (**10**). Intermolecular KIE values⁵⁰ between 1 and 2 are difficult to interpret, as they may signify the influence of (i) a non-selective hydrogen-abstracting agent, (ii) a more selective oxidant acting via a bent-transition state, or (iii) a rate-limiting step other than the C-H activation process. The KIE value of approximately 2⁵⁰ for the formation of the major product, adamantanone, has been frequently used to distinguish the active oxidant of Gif systems from the much more selective oxidant of the biological monooxygenases P-450 (KIE = 10–14;⁵¹ more modest values have also been reported²⁹) or sMMO^{25b} (KIE ≥ 50 for methane, 4 for ethane (*Methylosinus trichosporium*)⁵²), but also from the action of hydroxyl radicals, for which a value close to 1 is expected. Barton's interpretation¹ of this value invokes a side-on [2 + 2] approach of the C-H bond to the Fe=O unit in the transition state. However, the KIE value for adamantanone can be a composite of primary and secondary

Scheme 5



KIE and may also be influenced by the kinetics of activation of the second hydrogen atom.⁵³

To circumvent some of the limitations associated with the intermolecular KIE evaluation, we determined an intramolecular primary KIE for the tertiary position using adamantane-1,3-*d*₂ as substrate (Scheme 5).²⁹ This substrate, which is readily prepared²⁹ by deuteration (LiAlD₄) of commercially available 1,3-dibromoadamantane, has been successfully employed in KIE determinations²⁹ for oxygenations by P-450 model systems. Observing all critical corrections and precautions recommended in that elegant study²⁹ (especially with respect to the deuterium enrichment of the synthesized substrate (97.7(1) %), and the necessity to integrate over the entire GC-eluted peak of the unresolved products, composed of 1-adamantanol-*d*₂ and -*d*₁, in order to accurately evaluate (MS) the relative molecular ion content), we obtain a primary KIE value of 1.06(6) under N₂ and 1.73(2) under O₂ (4%) in N₂ for the oxygenation of adamantane to 1-adamantanol mediated by **2** (average of three trials). The KIE value obtained in the presence of N₂ is consistent with that expected for hydroxyl radical activity, while the higher value under low partial pressure of O₂ signifies that a more selective dioxygen-dependent oxidant (most likely, adamantyloxy radicals) is responsible for hydrogen-atom abstraction in conjunction with hydroxyl radicals. It is also reasonable to suggest that the intermolecular KIE value associated with the formation of 2-adamantanol (KIE = 1.46(3)) reflects mostly the contribution of the secondary KIE, which in the case of hydrogen-atom abstraction leading to carbon rehybridization can be as high as 1.4, as recently observed in FeCl₃-catalyzed oxidation of ethylbenzene by *t*-BuOOH.⁵⁴

(b) Gif Oxygenation of DMSO and DMSO/EtOH Competition Experiments. The generation of hydroxyl radicals in the course of Gif oxygenations was further investigated by employing a highly specific reaction of hydroxyl radicals, namely addition of HO• to DMSO ($k = 6.6 \times 10^9 \text{ M}^{-1} \text{ s}^{-1}$) to generate methanesulfinic acid and methyl radicals (eq 19).⁵⁵ The reaction favors addition of HO• to sulfur by a large margin (92%)^{55a} versus the alternative hydrogen-atom abstraction from the methyl group (8%).⁵⁶ The addition reaction is also strongly indicative of the presence of hydroxyl radicals, inasmuch as metal-oxo moieties are known to mediate oxygen atom transfer to sulfides⁵⁷ in the order R₂S → R₂S=O → R₂S(O)₂. However, to exclude the possibility that some other oxidant (especially iron (hydro)peroxo units⁵⁸) may be responsible for the same addition reaction, we chose to investigate the competition

(53) Hoffmann, P.; Robert, A.; Meunier, B. *Bull. Soc. Chim. Fr.* **1992**, 129, 85–97.

(54) (a) Merrigan, S. R.; Le Gloahec, V. N.; Smith, J. A.; Barton, D. H. R.; Singleton, D. A. *Tetrahedron Lett.* **1999**, 40, 3847–3850. (b) Singleton, D. A.; Thomas, A. A. *J. Am. Chem. Soc.* **1995**, 117, 9357–9358.

(55) (a) Veltwisch, D.; Janata, E.; Asmus, K.-D. *J. Chem. Soc., Perkin Trans. 2* **1980**, 146–153. (b) Urbanski, S. P.; Stickel, R. E.; Wine, P. H. *J. Phys. Chem. A* **1998**, 102, 10522–10529.

(56) Clement, J.-L.; Gilbert, B. C.; Ho, W. F.; Jackson, N. D.; Newton, M. S.; Silvester, S.; Timmins, G. S.; Tordo, P.; Whitwood, A. C. *J. Chem. Soc., Perkin Trans. 2* **1998**, 1715–1717.

(57) Mukerjee, S.; Stassinopoulos, A.; Caradonna, J. P. *J. Am. Chem. Soc.* **1997**, 119, 8097–8098.

(58) (a) Ho, R. Y. N.; Roelfes, G.; Feringa, B. L.; Que, L., Jr. *J. Am. Chem. Soc.* **1999**, 121, 264–265. (b) Kim, C.; Chen, K.; Kim, J.; Que, L., Jr. *J. Am. Chem. Soc.* **1997**, 119, 5964–5965.

(49) Barton, D. H. R.; Chabot, B. M.; Hu, B. *Tetrahedron* **1996**, 52, 10301–10312.

(50) Barton, D. H. R.; Doller, D.; Geletii, Y. V. *Tetrahedron Lett.* **1991**, 32, 3811–3814.

(51) (a) Sono, M.; Roach, M. P.; Coulter, E. D.; Dawson, J. H. *Chem. Rev.* **1996**, 96, 2841–2887. (b) Ortiz de Montellano, P. R. In *Cytochrome P-450: Structure, Mechanism, and Biochemistry*, 2nd ed.; Ortiz de Montellano, P. R., Ed.; Plenum Press: New York, 1995; pp 245–303. (c) Groves, J. T.; Han, Y.-Z. In *Cytochrome P-450: Structure, Mechanism, and Biochemistry*, 2nd ed.; Ortiz de Montellano, P. R., Ed.; Plenum Press: New York, 1995; pp 3–48.

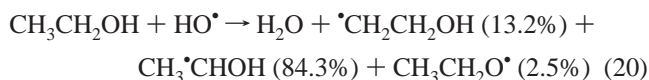
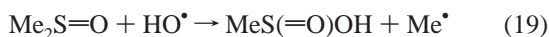
(52) (a) Nesheim, J. C.; Lipscomb, J. D. *Biochemistry* **1996**, 35, 5, 10240–10247. (b) Nesheim, J. C.; Lipscomb, J. D. *J. Inorg. Biochem.* **1995**, 59, 369.

Table 4. Product Profile of DMSO and DMSO/EtOH Oxidation by H₂O₂ Mediated by [Fe(Pic)₂(py)₂] (**2**)

Entry	Products (mmol)							Py-Me/ Py-EtOH
								
1 ^a	0.439	0.245	0.217					
2 ^b	0.191	0.105	0.093	0.066	0.043	0.010	0.004	3.16
3 ^c	0.169	0.088	0.064	0.070	0.048	0.011	0.005	2.40
4 ^d	0.129	0.072	0.060	0.074	0.058	0.013	0.006	1.73

^a General conditions unless otherwise noted; 0.2 mmol **2**; 2 mmol H₂O₂ (added by syringe pump over 6 hours at RT); DMSO (8.0 mL); py/AcOH (15.0/1.5 mL). ^b DMSO (8.8020 g, 112.6 mmol); EtOH (5.1149 g, 111.0 mmol). ^c DMSO (8.8070 g, 112.7 mmol); EtOH (6.6289 g, 143.9 mmol). ^d DMSO (8.8180 g, 112.8 mmol); EtOH (8.0220 g, 174.1 mmol).

kinetics of the underlying oxidant by coupling the DMSO addition reaction to hydrogen-atom abstraction from ethanol ($k = 1.9 \times 10^9 \text{ M}^{-1} \text{ s}^{-1}$)⁵⁹ (eq 20).



DMSO has been frequently used as an efficient trap of hydroxyl radicals generated from aqueous oxygenation systems.⁶⁰ Hydroxyl radicals are quantified by usually monitoring the accumulation of methanesulfinic acid by HPLC,^{60b} UV-vis⁶¹ or ion chromatography.^{60a} Quantification of methyl radicals by trapping with fluorescamine-derivatized nitroxyl radicals has also been reported.⁶² In the present study, the characteristic addition of alkyl radicals to protonated pyridine⁶³ permits facile quantification (by GC) of all carbon-centered radicals generated in eqs 19 and 20, provided that the reaction is performed under strictly inert atmosphere (argon) to avoid capturing of these radicals by dioxygen to the greatest possible extent. Furthermore, reactions with Fe(II) precursor reagents are solely entertained to minimize possible interference from the diffusion controlled oxidation of α -hydroxyethyl radicals to acetaldehyde by Fe(III) sites (eq 21).^{45,64} Fortunately, as mentioned above, Fe(III) Pic species reductively decompose to their Fe(II) congeners in the presence of H₂O₂.

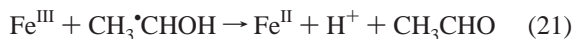
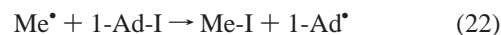


Table 4 summarizes the results of several Gif oxygenation experiments mediated by **2** (0.2 mmol) in py/AcOH (15.0/1.5 mL) in the presence of DMSO or DMSO/EtOH (various relative concentrations). In the presence of DMSO (entry 1), 2-, 3-, and 4-picoline are obtained, as expected for the addition of the

methyl radical (the least selective and least nucleophilic of all alkyl radicals⁶⁵) to all aromatic positions of pyridine and/or protonated pyridine. Traces of methylated bipyridines are also detected by GC-MS. Addition of EtOH to the reaction mixture at various increasing concentrations versus DMSO (entries 2-4) causes progressive reduction of the amounts of all picolines and concomitant augmentation of the amounts of pyridine-trapped hydroxyethyl radicals. As observed in the case of adamantyl radicals, these latter ethanol-derived radicals add exclusively at positions 2- and 4- of pyridine, owing to the high rate and regioselectivity of addition of carbon-centered radicals to protonated (rather than non-protonated) pyridine, both increasing with the nucleophilicity of the alkyl radical.⁴⁵ From the ratio of pyridine-captured methyl over hydroxyethyl radicals and knowledge of the relative concentrations of DMSO and EtOH, a ratio of rate constants $k_{\text{EtOH}}/k_{\text{DMSO}}$ of 0.34(3) is calculated, which is in reasonable agreement with that reported from pulse radiolysis experiments ($k_{\text{EtOH}}/k_{\text{DMSO}} = 0.29$).⁵⁹ Furthermore, the internal competition for hydrogen-atom abstraction from the α - and β -carbon atoms of EtOH, as judged by the ratio py-CH(CH₃)OH/py-CH₂CH₂OH, yields a selectivity of 7.3(4) which is not unlike that documented by radiation chemistry⁶⁵ (eq 20), considering the uncertainty in determining the low-yield py-CH₂CH₂OH products. The qualitative results and quantitative estimates of the experiments presented in this section strongly support the involvement of hydroxyl radicals as major oxidant in Gif-type oxygenations.

(c) Gif Oxygenations in the Presence of 1-Iodoadamantane. To ascertain that the formation of picolines observed in the oxygenation of DMSO by Gif reagents is due to generation of methyl radicals via eq 19, the reaction of HO[•] with DMSO was coupled to the well documented methyl radical abstraction of iodine atoms from alkyl iodides,⁶⁶ conveniently applied to 1-iodoadamantane⁶⁷ (eq 22). Similar reaction sequences have been introduced by Minisci⁶⁸ for the preparative scale synthesis of alkylpyridines in the presence of protonated *N*-heterocycles. Hydroxyl radicals were provided in those experiments by Fenton reagents.



A typical Gif oxygenation of DMSO (8 mL) by H₂O₂ (2 mmol) mediated by **2** (0.2 mmol) in the presence of 1-iodoadamantane (5 mmol) in py/AcOH (15.0/1.5 mL) under argon affords cleanly 2-(1-Ad)py (0.55 mmol) and 4-(1-Ad)py (0.44 mmol), as well as trace amounts of 1-Ad-OH. No picolines are detected, suggesting that the methyl radicals, generated via reaction 19 in amounts commensurating with those observed in the absence of 1-Ad-I, are predominantly diverted toward iodine abstraction and 1-Ad[•] formation (eq 22).

Under the same experimental conditions, but in the absence of DMSO, the two *tert*-adamantylpyridines are still observed in lower yields (2-(1-Ad)py: 0.16 mmol; 4-(1-Ad)py: 0.13 mmol), accompanied by a host of other products. Those have been identified, but not quantified, by GC-MS and include iodopyridines, four diiodoadamantanes (1,2-I₂-Ad (racemic), 1,3-I₂-Ad, 1,4-I₂-Ad (two diastereomers)), and eight 1-iodo-

(59) Buxton, G. V.; Greenstock, C. L.; Helman, W. P.; Ross, A. B. *J. Phys. Chem. Ref. Data* **1988**, *17*, 513-886.

(60) (a) Yurkova, I. L.; Schuchmann, H.-P.; von Sonntag, C. *J. Chem. Soc., Perkin Trans. 2* **1999**, 2049-2052. (b) Daniels, J. S.; Gates, K. S. *J. Am. Chem. Soc.* **1996**, *118*, 3380-3385.

(61) Steiner, M. G.; Babbs, C. F. *Arch. Biochem. Biophys.* **1990**, *278*, 478-481.

(62) Li, B.; Gutierrez, P. L.; Blough, N. V. *Anal. Chem.* **1997**, *69*, 4295-4302.

(63) Minisci, F.; Vismara, E.; Fontana, F.; Morini, G.; Serravalle, M.; Giordano, C. *J. Org. Chem.* **1987**, *52*, 730-736.

(64) Minisci, F.; Citterio, A.; Vismara, E. *Tetrahedron* **1985**, *41*, 4157-4170.

(65) Asmus, K.-D.; Möckel, H.; Henglein, A. *J. Phys. Chem.* **1973**, *77*, 1218-1221.

(66) Hawari, J. A.; Kanabus-Kamiuska, J. M.; Wayner, D. D. M.; Griller, D. In *Substituent Effects in Radical Chemistry*; Viehe, H. G., Ed.; Reidel Publishing Company: Dordrecht, 1986; pp 91-107.

(67) Ryu, I.; Yamazaki, H.; Ogawa, A.; Kambe, N.; Sonoda, N. *J. Am. Chem. Soc.* **1993**, *115*, 1187-1189.

(68) Fontana, F.; Minisci, F.; Vismara, E. *Tetrahedron Lett.* **1988**, *29*, 1975-1978.

adamantyl-pyridine coupled products (most likely due to addition of the three possible 1-I-Ad* radicals to positions 2- and 4- of pyridine, including two pairs of diastereomers). All products are well understood and arise from initial hydroxyl-radical addition to pyridine^{59,69} and hydrogen-atom abstraction from 1-iodoadamantane, generating carbon-centered radicals. These in turn perform iodine-atom abstraction from 1-iodoadamantane and/or coupling with protonated pyridine. With the exception of the *tert*-adamantylpyridines, all other products are reduced to trace amounts in the presence of DMSO (8 mL, 113 mmol) as previously noted. Similarly, formation of these products is inhibited to a lesser extent in the presence of EtOH (8 mL, 136 mmol). These results further confirm that the active oxidant involved initiates genuine radical chemistry under Gif conditions.

(d) Miscellaneous Control Experiments. As an additional test of the viability of the Fe^{IV}=O hypothesis we attempted to oxygenate adamantane (5 mmol) by the oxo donor reagent 2,6-dimethyl-1-iodosylbenzene (2 mmol) in the presence of **2** in py/AcOH (30.0/3.0 mL) under argon. Not even traces of oxo products or adamantylpyridines were observed. Although the experiment does not conclusively negate the action of Fe^{IV}=O units, as it is not known whether coordinated pyridine can be easily replaced by the oxo donor moiety,⁷⁰ it is nevertheless supportive of the main conclusion of the present study.

Finally, we note that attempts to generate authentic hydroxyl radicals in py/AcOH in the presence of adamantane, by continuous UV photolysis of H₂O₂⁷¹ (by means of a high-pressure xenon lamp, 75 W), afforded product profiles which demonstrate the usual partitioning of adamantyl radicals between dioxygen and protonated pyridine. However, the high *tert*/*sec* selectivities obtained even under a constant stream of argon ($3^\circ/2^\circ \approx 10$), and the yellowing of the reaction solutions, suggested that other less indiscriminate radical species generated during photolysis (most likely derivatives of pyridinyl radicals⁷²) interfere with the outcome of this control experiment.

Further Discussion and Conclusions

Early reports of Gif chemistry by D. H. R. Barton and co-workers¹ were centered on the oxygenation of adamantane as a mechanistic probe of what was perceived to be a non-radical pathway for the activation of hydrocarbons. Initial product profiles largely favored (*sec*/*tert* = 22)⁷³ the formation of secondary adamantyl oxo products (particularly 2-one) over 1-adamantanol. The subsequent addition of *tert*-adamantylpyridines (but not *sec*-adamantylpyridines) to the product profile reduced the *sec*/*tert* selectivity to approximately 1.1.⁷⁴ These values had not been corrected on a per-hydrogen basis at the time, thus concealing the actual preponderance of tertiary over secondary C–H activation (*tert*/*sec* = 2.7) in adamantane oxidations. This selectivity is only slightly higher than what would be expected from the action of the indiscriminate hydroxyl radicals.⁷⁵ This point was not taken into account, as

comparisons were made¹ with systems in which much more selective oxygen-centered radicals were operating.⁷⁶ These and many other inconsistencies and fallacies in the interpretation of Gif chemistry have been summarized in an insightful review by M. J. Perkins²² to which the reader is referred.

Nevertheless, adamantane was perceived by Barton² as an exception to the application of an all pervasive non-radical mechanism, since the formation of *tert*-adamantyl radicals could not be denied in light of the presence of *tert*-adamantylpyridines. The argument was thus reduced to the applicability of the non-radical activation path to the secondary C–H positions, for which no *sec*-adamantylpyridines were detected. These conclusions were further supported by the competition experiments²⁶ noted above, indicating that the degree of partitioning of genuine tertiary and secondary adamantyl radicals between dioxygen (4%) and protonated pyridine differed from what was obtained in Gif^V-type chemistry. Two observations which should have caused concern about the validity of these control experiments are (i) the discrepancy of the numerical values even for the tertiary adamantyl radicals, and (ii) that the amounts of *sec*-adamantylpyridines produced in the Gif experiment were small, but not zero. A major finding of the present work is that, under inert atmosphere, *sec*-adamantylpyridines can be readily detected in good yields in Gif oxygenations of adamantane by H₂O₂. Moreover, the analogous competition experiments involving authentic adamantyl radicals, when conducted under conditions permitting genuine comparison with the Gif experiment, provide partitioning values which are very similar to those obtained in Gif chemistry. It is possible that the high *sec* Ad(O)/Ad-py value (~94) obtained by Barton²⁶ via a Gif^V-type reagent (FeCl₂/Zn/O₂ (4%)), if not erroneous, may be due to the reductive environment of this system. As suggested by Minisci,⁴⁶ these conditions may not be as effective as the Barton PTOC esters in inducing oxidative rearomatization to generate *sec*-adamantylpyridines. We have also noted that static delivery of O₂ (4%)/N₂ in the headspace of the Gif reaction tends to increase the amount of *tert*-adamantylpyridines at the expense of 1-ol, probably due to O₂ depletion. The presence of Zn, which is known⁷⁷ to reduce O₂ to superoxide in py/AcOH, may contribute to this effect. The present results provide strong evidence that the product profile of Gif oxygenation of adamantane is dictated by the generation of diffusively free *tert*- and *sec*-adamantyl radicals.

Newcomb's results²³ on the oxidation of the radical-clock substrate 1-methyl-2-phenylcyclopropane by the Gif reagent FeCl₃/H₂O₂ provided the first strong indication that diffusively free alkyl radicals are generated in Gif solutions. Indeed, the entire product profile was derived from the rapidly rearranging ($k = 3 \times 10^{11} \text{ s}^{-1}$ (ring opening)), free (2-phenyl-cyclopropyl)-carbonyl radical, and no products were observed from insertion into the methyl C–H bonds of the unrearranged substrate. These results were interpreted by Barton⁷⁸ as an exceptional case, similar to that observed for the tertiary position of adamantane, in which a putative Fe^V–R bond supposedly collapses to Fe^{IV} and R*. The present work shows that there is nothing special

(69) (a) Cercek, B.; Ebert, M. *Trans. Faraday Soc.* **1967**, *63*, 1687–1698. (b) Steenken, S.; O'Neill, P. *J. Phys. Chem.* **1978**, *82*, 372–374.

(70) For reservations concerning the intermediacy of metal-oxo units in oxygenations mediated by iodosylbenzene derivatives see: Nam, W.; Valentine, J. S. *J. Am. Chem. Soc.* **1993**, *115*, 1772–1778.

(71) (a) Nadezhdin, A.; Dunford, H. B. *J. Phys. Chem.* **1979**, *83*, 1957–1961. (b) Livingston, R.; Zeldes, H. *J. Chem. Phys.* **1966**, *44*, 1245–1259.

(72) Kosower, E. M. In *Free Radicals in Biology*; Pryor, W. A., Ed.; Academic Press: New York, 1976; pp 1–53.

(73) Barton, D. H. R.; Gastiger, M. J.; Motherwell, W. B. *J. Chem. Soc., Chem. Commun.* **1983**, 41–43.

(74) Balavoine, G.; Barton, D. H. R.; Boivin, J.; Lecoupanec, P.; Lelandais, P. *New J. Chem.* **1989**, *13*, 691–700.

(75) (a) Buxton, G. V.; Greenstock, C. L.; Helman, W. P.; Ross, A. B. *J. Phys. Chem. Ref. Data* **1988**, *17*, 513–886. (b) Baker, R. R.; Baldwin, R. R.; Walker, R. W. *Trans. Faraday Soc.* **1970**, *66*, 2812–2826. (c) Russell, G. A. In *The Chemistry of Alkanes and Cycloalkanes*; Patai, S., Rappoport, Z., Eds.; Wiley: New York, 1992; pp 966–983. (d) Kochi, J. K. In *Free Radicals*; Kochi, J. K., Ed.; Wiley: New York, 1973; Vol. II, pp 689–690.

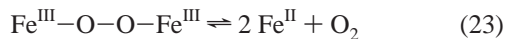
(76) Fossey, J.; Lefort, D.; Massoudi, M.; Nedelec, J.-Y.; Sorba, J. *Can. J. Chem.* **1985**, *63*, 678–680.

(77) Sawyer, D. T. *Oxygen Chemistry*; Oxford University Press: New York, 1991; pp 120–187.

(78) Barton, D. H. R. Personal communication.

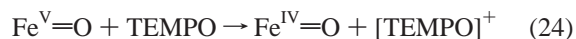
about the tertiary position of adamantane, and the same should also apply to the radical-clock substrates. Furthermore, there is no evidence to support that high-valent Fe=O units are involved as active oxidants in Gif chemistry (*vide infra*). An even earlier report by Perkins,⁸ in which a Gif oxidation of cyclohexane led to detection of cyclohexyl radicals by spin-trapping, did not receive its due recognition at the time, and was dismissed as an overly qualitative result.

Preliminary results of the present work have also been criticized by Barton⁷⁸ as indicating operation of Fe(II)/H₂O₂ dependent cycles ("Fe^{II}/Fe^{IV} radical manifold"; eqs 7, 8), even in cases in which ferric reagents are employed as catalyst precursors under scrupulous argon purging. This argument is associated with the late introduction³ of two manifolds, the radical noted above, and the original Fe^{III}/Fe^V non-radical manifold. The distinction was most likely introduced once it was realized³ that Fe(II)/H₂O₂ based Gif oxygenations of cyclohexane produce cyclohexyl chloride (in the presence of Cl⁻) or cyclohexylpyridines (in the absence of Cl⁻), both indicating the presence of cyclohexyl radicals, while Fe(III)/H₂O₂ Gif reagents mostly produce cyclohexanone and cyclohexanol, assumed to indicate non-radical pathways. An important addendum to this observation was that, the Fe(II)/H₂O₂ system starts producing more oxo products under an oxygen stream, while the Fe(III)/H₂O₂ system starts generating cyclohexyl chloride in the presence of Cl⁻ under an argon stream. While these important results can be explained in a straightforward manner as consistent with the generation and partitioning of cyclohexyl radicals among O₂ > Fe^{III}-Cl > [pyNH]⁺ under all conditions, they were perceived³ instead as indicating interconversion of the two manifolds via reversible loss of dioxygen⁷⁹ from a putative diferric peroxo unit (eq 23).



The present results refute the double manifold theory at various levels of consideration, without disputing the fact that all reagents examined most likely produce their active oxidant via Fe(II)/H₂O₂ interactions. First, the product profiles of adamantane oxygenations clearly illustrate that *tert*- and *sec*-adamantyl radicals are produced by both Fe(II)/H₂O₂ and Fe(III)/H₂O₂ systems, even for Fe(III) reagents such as Fe(Pic)₃ which have been extensively used in Barton's experiments.^{3,80} The amounts of *sec*-adamantylpyridines are indeed reduced when Fe(III)/H₂O₂ systems are applied, but this is simply due to the increased *in situ* production of O₂ by these systems. Notable is also the generation of 2-chloroadamantane at the expense of *sec*-adamantylpyridines in the presence by FeCl₃/H₂O₂ in py/AcOH, a ferric reagent which has also been routinely used by Barton.³ Most importantly, the results from Gif oxygenations of adamantane in the presence of TEMPO and the related competition experiments, show clearly that generation of *tert*- and *sec*-adamantyl radicals dictates the product profile *even under pure O₂*. The formation of TEMPO-trapped *sec*-alkyl radicals had been noted by Barton,⁴⁹ but because *sec*-alkylpyridines had not been observed in related experiments, it was hypothesized⁴⁹ that the generation of alkyl radicals was induced by TEMPO via one electron-reduction of the putative Fe^V=O oxidant of the non-radical manifold to the corresponding Fe^{IV}=O oxidant of the radical manifold (eqs 24 and 7-8). This

circuitous interpretation is not supported by the results of the present study, since adamantyl radicals are clearly present even in the absence of TEMPO.



The most compelling evidence against the double radical manifold is the realization that HO• radicals play a major role in H-abstraction and addition reactions of Gif chemistry. The high-valent Fe^{IV/V}=O units proposed by Barton³ have always been suspected on account of the widely differing product profiles obtained by Gif reagents (C-H and C=C ketonation) versus those realized with biological monooxygenases^{51,81} (C-H insertion to form alcohols; C=C epoxidation). The involvement of hydroxyl radicals has been inferred in the present study by virtue of diagnostic reactions, chief among which is their highly specific addition of HO• to DMSO to afford pyridine-trapped methyl radicals under Gif conditions. Competitive interception of hydroxyl radicals by DMSO and EtOH confirms that the competition kinetics are consistent with the presence of this oxidant rather than some other active species generated in Gif solutions. The low *tert/sec* selectivity values and the intramolecular KIE value close to unity, obtained under argon, are also typical of HO• kinetics.⁷⁵ Under increasing amounts of dioxygen a more selective oxidant, most likely substrate-centered alkoxy radicals,²² may contribute to the hydrogen-abstracting process, as judged by the increased *tert/sec* selectivity and magnitude of the intramolecular KIE value. These results also reverse scepticism expressed in our previous publication⁷ in regards to the role of hydroxyl radicals in Gif chemistry, although a handful of product profile discrepancies noted in that study need to be revisited. In retrospect, we recognize that the Gif^{IV}-type systems previously employed are unsuitable for detailed mechanistic work due to complications introduced by the obligatory presence of O₂/Zn. As noted above, O₂ increases the selectivity of Gif reagents, most likely by increasing the contribution of substrate-centered alkoxy radicals versus hydroxyl radicals. Thus, typical features of hydroxyl radical chemistry, such as hydroxylation of aromatics, are suppressed. In addition, O₂ conceals the presence of *sec*-alkyl radicals. As indicated in the present study, Zn powder also increases the selectivity of the Gif reaction, probably via selective reduction of the oxygen-centered radicals. The heterogeneity of the Gif solutions introduced by Zn is another source of concern; notably, mass balances are inferior in the presence of Zn. These limitations are all circumvented with the present homogeneous Fe/H₂O₂ combinations which permit addition of O₂ at will, therefore assisting in unravelling the underlying nature of Gif chemistry.

It should also be noted that M. J. Perkins was the first to pinpoint in an early report⁸ that the *p*-hydroxylation of phenylalanine by an Fe(III)/H₂O₂ reagent is consistent with the action of HO• radicals. More recently, M. J. Perkins²² has also drawn attention to the well-documented Gif oxidation of pyridine to hydroxypyridines and bipyridines, as another instance of hydroxyl radical attack. Some controversy with respect to the regioselectivity of pyridine hydroxylation in Gif chemistry (which also gives some 3-HOpy, as expected for the electrophilic HO•) and by photolytically generated HO• radicals (reportedly²⁷ producing 2-HOpy and 4-HOpy in a ratio of 2:1) need to be eventually reconciled. Furthermore, hydroxylation of aromatic moieties by Gif reagents has been detected by M. Newcomb,²³ who has also noted that the absence of molecular selectivity in

(79) Kitajima, N.; Tamura, N.; Amagai, H.; Fukui, H.; Moro-oka, Y.; Mizutani, Y.; Kitagawa, T.; Mathur, R.; Heerwegh, K.; Reed, C. A.; Randall, C. R.; Que, L., Jr.; Tatsumi, K. *J. Am. Chem. Soc.* **1994**, *116*, 9071-9085.

(80) Barton, D. H. R.; Beck, A. H.; Delanghe, N. C. *Tetrahedron Lett.* **1996**, *37*, 1555-1558.

(81) (a) Wallar, B. J.; Lipscomb, J. D. *Chem. Rev.* **1996**, *96*, 2625-2657. (b) Feig, A. L.; Lippard, S. J. *Chem. Rev.* **1994**, *94*, 759-805.

competitive Gif oxygenations of cycloalkanes⁸² can be consistent with H-atom abstraction by hydroxyl radicals.⁸³ Notably, Barton¹ frequently used to refer to the beneficial role of pyridine in Gif chemistry in trapping any residual hydroxyl radicals.

Can there be an additional active oxidant responsible for the chemistry observed in the current investigation? For unfunctionalized alkanes, the answer is largely negative. Preliminary oxygenation experiments of *cis*-stilbene by H₂O₂ mediated by **2** or **10** in py/AcOH or CH₃CN/AcOH indicate that the product profile is mostly composed of benzaldehyde, deoxybenzoin, *trans*-stilbene oxide, and *cis*-stilbene oxide (especially in CH₃CN/AcOH). While the former two products can be readily generated via hydroxyl-radical addition to the double bond⁸⁴ (although other mechanisms involving electron transfer from alkenes to metal oxo reagents have also been discussed⁸⁵), stilbene epoxides may instead originate from oxo transfer processes.⁸⁶ High-valent iron-oxo units⁸⁷ need not be invoked, since iron (hydro)peroxo species (Fe^{III}–OO(H))⁸⁸ may be efficient oxo donor moieties,⁸⁹ as also indicated in recent reconsiderations of the role of the active oxidants in P-450 oxygenations.⁹⁰ These Fe^{IV/III}–OOH species may also be the immediate precursors of hydroxyl radicals, although the importance of the different oxidation states of iron in these units

(82) Barton, D. H. R.; Launay, F.; Le Gloahec, V. N.; Li, F.; Smith, F. *Tetrahedron Lett.* **1997**, *38*, 8491–8494.

(83) Newcomb, M.; Simakov, P. A. *Tetrahedron Lett.* **1998**, *39*, 965–966.

(84) (a) von Sonntag, C. *The Chemical Basis of Radiation Biology*; Taylor & Francis: London, 1987; pp 37–38. (b) von Sonntag, C.; Schuchmann, H.-P. *Angew. Chem., Int. Ed. Engl.* **1991**, *30*, 1229–1253.

(85) (a) Gross, Z.; Nimri, S. *J. Am. Chem. Soc.* **1995**, *117*, 8021–8022. (b) Traylor, T. G.; Miksztal, A. R. *J. Am. Chem. Soc.* **1987**, *109*, 2770–2774.

(86) Ostovic, D.; Bruice, T. C. *Acc. Chem. Res.* **1992**, *25*, 314–320.

(87) (a) Groves, J. T.; Nemo, T. E. *J. Am. Chem. Soc.* **1983**, *105*, 5786–5791. (b) Castellino, A. J.; Bruice, T. C. *J. Am. Chem. Soc.* **1988**, *110*, 158–162. (c) Castellino, A. J.; Bruice, T. C. *J. Am. Chem. Soc.* **1988**, *110*, 7512–7519.

(88) Sam, J. W.; Tang, X.-J.; Peisach, J. *J. Am. Chem. Soc.* **1994**, *116*, 5250–5256.

(89) Murugesan, N.; Hecht, S. M. *J. Am. Chem. Soc.* **1985**, *107*, 493–500.

(90) (a) Newcomb, M.; Shen, R.; Choi, S.-Y.; Toy, P. H.; Hollenberg, P. F.; Vaz, A. D. N.; Coon, M. J. *J. Am. Chem. Soc.* **2000**, *122*, 2677–2686. (b) Toy, P. H.; Newcomb, M.; Coon, M. J.; Vaz, A. D. N. *J. Am. Chem. Soc.* **1998**, *120*, 9718–9719.

needs to be better defined. The stoichiometry of the Fenton reaction is better served by assuming an Fe^{II}–OOH precursor of hydroxyl radicals and an Fe^{III}–OOH precursor of hydroperoxyl radicals. In contrast, recent studies¹¹ of iron-based ROOH-supported (R = H, *t*-Bu) oxygenation of substrates favor homolytic cleavage of the O–O bond in Fe^{III}–OOR precursor species as the source of HO•/RO• radicals. The latter mode of decomposition, which may be influenced by the strength of the ligand field,^{58a} has been documented with the assistance of Co^{III}–OOR model species in a thorough study.⁹¹ Future investigations are directed toward unraveling those metal-centered (hydro)peroxo intermediates which may be the immediate precursors of hydroxyl radicals and possibly active oxo donors to olefinic substrates.

Acknowledgment. We thank Corina E. Rogge and Professor John P. Caradonna for a sample of 2,6-dimethyl-1-iodosylbenzene and fruitful discussions. Patricia C. Ong and Remle Çelenligil-Çetin are also acknowledged for offering valuable experimental assistance. We also thank Dr. Andrew Tyler for assisting in obtaining electrospray ionization mass spectra and Michael Creech for providing GC–MS data. The present work was generously supported by grants from the U.S. Environmental Protection Agency (R823377-01-1) and the donors of the Petroleum Research Fund administered by the ACS (ACS-PRF-29383-G3), and in part by a grant from the Division of Chemical Sciences, Office of Basic Energy Sciences, Office of Science, U.S. Department of Energy (DE-FG02-99ER14978).

Supporting Information Available: ORTEP diagrams and Tables 1–35 containing listings of crystal data and structure refinement, atomic coordinates and equivalent isotropic displacement parameters, interatomic distances and bond angles, anisotropic displacement parameters, and hydrogen coordinates and isotropic displacement parameters for compounds **3**, **5–7**, and **9–11** (PDF). X-ray crystallographic file in CIF format. This material is available free of charge via the Internet at <http://pubs.acs.org>.

JA000063H

(91) Chavez, F. A.; Rowland, J. M.; Olmstead, M. M.; Mascharak, P. K. *J. Am. Chem. Soc.* **1998**, *120*, 9015–9027.